

PROMOTION PERMUTATIONS FOR TABLEAUX

CHRISTIAN GAETZ, OLIVER PECHENIK, STEPHAN PFANNERER, JESSICA STRIKER,
AND JOSHUA P. SWANSON

ABSTRACT. In our companion paper [GPPSS23a], we develop a new SL_4 -web basis. Basis elements are given by certain planar graphs and are constructed so that important algebraic operations can be performed diagrammatically. A guiding principle behind our construction is that the long cycle $(12 \dots n) \in \mathfrak{S}_n$ should act by rotation of webs. Moreover, the bijection between webs and tableaux should intertwine rotation with the promotion action on tableaux.

In this paper, we develop necessary notions of *promotion permutations* and *promotion matrices*, which are new even for standard tableaux. To support inductive arguments in [GPPSS23a], we must however work in the more general setting of *fluctuating tableaux*, which we introduce and which subsumes many classes of tableaux that have been previously studied, including (generalized) oscillating, vacillating, rational, alternating, and (semi)standard tableaux. Therefore, we also give here a full development of the basic combinatorics and representation theory of fluctuating tableaux.

1. INTRODUCTION

Tableaux are elementary, yet powerful, objects. They are defined simply as ‘numbers in boxes with rules,’ yet they are central objects in algebraic combinatorics. Tableaux exhibit excellent properties from many perspectives, including enumerative (hook and Jacobi–Trudi formulas), algebraic (plactic monoid, crystals), dynamical (promotion, evacuation), and representation-theoretic (bases of Specht and Schur modules, etc.). Many of the most important families of tableaux are permuted by the action of a *promotion* operator (see, e.g., [Sch72, Pec14, Pat19]), which will be our main focus in this paper. While promotion on tableaux of an arbitrary-shaped partition may have large order, an amazing fact is that promotion on various types of rectangular tableaux has order dividing n , the maximum allowed entry. This is not only true for standard and semistandard Young tableaux (see, e.g., [Hai92, Rho10]), but also for *generalized oscillating* tableaux [Pat19].

Our motivation for this project comes from combinatorial representation theory. Specifically, in the companion paper [GPPSS23a] we develop a new rotation-invariant *web basis* for the Specht module $S^{(d^4)}$, building on analogous constructions for $S^{(d^2)}$ (see [TL71, KR84]) and $S^{(d^3)}$ [Kup96]. Web bases have basis elements given by certain planar graphs and are constructed in such a way that important algebraic operations can be carried out diagrammatically. A guiding principle behind our new construction in [GPPSS23a] is that the long cycle $c = (1\ 2 \dots n) \in \mathfrak{S}_n$ should act (up to signs) on basis elements as the permutation given by rotation of planar graphs. Moreover, the key bijection between web diagrams and tableaux should carry the action of rotation to the promotion action on tableaux.

To carry out this program, we need to develop notions of *promotion permutations* and *promotion matrices*. These ideas are the main contribution of the current paper and are new even in the case of standard tableaux. For the sake of being able to make inductive arguments in [GPPSS23a],

Date: July 4, 2023.

Gaetz was partially supported by a Klarman Postdoctoral Fellowship at Cornell University and by an NSF Postdoctoral Research Fellowship (DMS-2103121). Pechenik was partially supported by a Discovery Grant (RGPIN-2021-02391) and Launch Supplement (DGEER-2021-00010) from the Natural Sciences and Engineering Research Council of Canada. Pfannerer was partially supported by the Austrian Science Fund (FWF) P29275 and is a recipient of a DOC Fellowship of the Austrian Academy of Sciences. Striker was partially supported by a Simons Foundation/SFARI grant (527204, JS) and NSF grant DMS-2247089.

we need however to work in a setting that generalizes Patrias’ generalized oscillating tableaux. To avoid the monstrous name ‘generalized generalized oscillating tableaux,’ we propose the new name *fluctuating tableaux* for this class (see Definition 2.1) and work in that generality throughout this paper. As discussed in Remark 8.19, fluctuating tableaux subsume many classes of tableaux that have been previously studied, including standard, dual semistandard, oscillating, generalized oscillating, vacillating, rational, and alternating tableaux.

Our main construction associates a *promotion matrix* to a fluctuating tableau of general shape. Indeed, we give six different characterizations of this construction:

- (1) Bender–Knuth involution swap positions (see Definition 5.14),
- (2) decorated local rule diagrams (see Proposition 5.19),
- (3) row slides in jeu de taquin (see Proposition 6.9),
- (4) antiexcedance sets (see Theorem 6.12),
- (5) first balance point conditions (see Proposition 8.22), and
- (6) a Kashiwara crystal raising algorithm (see Theorem 8.24).

When the shape is rectangular of r rows, we further transform the promotion matrix to an $(r-1)$ -tuple $(\mathbf{prom}_1, \dots, \mathbf{prom}_{r-1})$ of *promotion permutations*. The tableau may be uniquely reconstructed from its promotion permutations. For example, for a standard tableau T , the values appearing in the first i rows are exactly the antiexcedances of the permutation \mathbf{prom}_i . Our main result, Theorem 6.7, establishes important structural properties of these permutations, which are critical to the companion paper [GPPSS23a] and also likely of independent interest. We also show in Theorem 6.5 that promotion has order dividing n even in the rectangular fluctuating setting, unifying various special cases appearing throughout the literature on promotion.

For $r = 2$, \mathbf{prom}_1 is the involution seen diagrammatically as the noncrossing matching corresponding to the 2-row standard Young tableaux via the usual Catalan bijection (see, e.g., [Sta99, Tym12]). The promotion permutation \mathbf{prom}_1 of a 3-row rectangular standard Young tableaux was defined and studied in [HR22], where it was further noted that \mathbf{prom}_2 could also be defined, but that it would necessarily be the inverse of \mathbf{prom}_1 . We show in Theorem 6.7 these properties hold more generally for rectangular fluctuating tableaux with an arbitrary number r of rows: \mathbf{prom}_i is always the inverse of \mathbf{prom}_{r-i} , and, when r is even, $\mathbf{prom}_{r/2}$ is a fixed-point free involution. Theorem 6.12 shows that the antiexcedances of the promotion permutations determine the entries of the corresponding tableau.

We give an example of promotion permutations for a rectangular standard Young tableau below. Precise definitions appear later in the paper.

Example 1.1. Consider the standard Young tableau below. Its promotion permutations in one-line notation are shown, with the antiexcedances highlighted in blue.

$$E = \begin{array}{|c|c|c|c|} \hline 1 & 2 & 5 & 6 \\ \hline 3 & 4 & 7 & 10 \\ \hline 8 & 9 & 11 & 14 \\ \hline 12 & 13 & 15 & 16 \\ \hline \end{array} \quad \begin{array}{l} \mathbf{prom}_1(E) = 4 \ 3 \ 14 \ 10 \ 9 \ 7 \ 8 \ 16 \ 13 \ 11 \ 12 \ 6 \ 5 \ 15 \ 2 \ 1 \\ \mathbf{prom}_2(E) = 14 \ 9 \ 16 \ 15 \ 11 \ 8 \ 13 \ 6 \ 2 \ 12 \ 5 \ 10 \ 7 \ 1 \ 4 \ 3 \\ \mathbf{prom}_3(E) = 16 \ 15 \ 2 \ 1 \ 13 \ 12 \ 6 \ 7 \ 5 \ 4 \ 10 \ 11 \ 9 \ 3 \ 14 \ 8 \end{array}$$

The reader may check that the permutations $\mathbf{prom}_1(E)$ and $\mathbf{prom}_3(E)$ are inverses of each other and that $\mathbf{prom}_2(E)$ is a fixed-point free involution. Note also that the antiexcedances of $\mathbf{prom}_i(E)$ are exactly the entries in the first i rows of E .

Section 7 illustrates our main results, Theorems 6.5 and 6.7, by showing in Corollary 7.1 that promotion and evacuation act as rotation and reflection on promotion permutation diagrams. This yields a dihedral model of promotion and evacuation on rectangular fluctuating tableaux (see Example 7.2). These diagrams are new even for standard tableaux.

Section 8 gives a crystal-theoretic interpretation of the purely combinatorial results of the preceding sections. The main result (Theorem 8.24) is a crystal raising algorithm to compute promotion

permutations and matrices. We also use crystal techniques to prove the balance point characterization, Proposition 8.22.

The rest of this paper is devoted to proving many other beautiful properties of tableaux in the fluctuating setting, such as interpretations of promotion via growth diagrams (Section 3), Bender-Knuth involutions (Section 4.1), jeu de taquin (Section 4.4), and crystals (Section 8). Much of this material is known to experts in the semistandard setting. However, even for semistandard tableaux, it is hard or impossible to find explicit proofs in the literature for many of these facts. We hope that in giving the technicalities needed for the general fluctuating case, our paper can also serve as a useful compendium of these details in more traditional settings.

This paper is organized as follows. Section 2 defines fluctuating tableaux and relates these tableaux to representation theory. Sections 3 and 4 give rigorous proofs of many standard facts about tableaux at the level of generality of fluctuating tableaux. In Sections 5 and 6, we move to ideas that are new even for standard Young tableaux: promotion matrices, promotion permutations, and their properties. Section 7 applies promotion permutations to give a dihedral model of promotion and evacuation for rectangular fluctuating tableaux. Section 8 relates the constructions of this paper to Kashiwara's theory of crystals.

An extended abstract describing part of this work appears in the proceedings of FPSAC 2023 [GPPSS23b].

2. FLUCTUATING TABLEAUX

Here we define fluctuating tableaux, describe their connections to representation theory, and introduce some associated basic combinatorial notions.

2.1. Generalized partitions and fluctuating tableaux. A *generalized partition* with r rows is a tuple $\lambda = (\lambda_1, \dots, \lambda_r) \in \mathbb{Z}^r$ where $\lambda_1 \geq \dots \geq \lambda_r$. We visualize generalized partitions as *diagrams*, which are semi-infinite collections of *cells* (or *boxes*) as in Figure 1. (Stembridge [Ste87] refers to generalized partitions as *staircases*; we prefer to avoid potential confusion with *staircase partitions* $(k, k-1, \dots, 1)$.)

Let \mathcal{A}_r be the collection of subsets of $\{\pm 1, \dots, \pm r\}$ whose elements are all of the same sign. We write \mathbf{e}_i for the i -th standard basis vector of \mathbb{Z}^r . If $S \in \mathcal{A}_r$ is a positive subset of $\{\pm 1, \dots, \pm r\}$, we define $\mathbf{e}_S = \sum_{i \in S} \mathbf{e}_i$, while if S is a negative subset, we define $\mathbf{e}_S = -\sum_{i \in S} \mathbf{e}_{-i}$. We say two r -row generalized partitions λ, μ *differ by a skew column* if $\lambda = \mu + \mathbf{e}_S$ for some $S \in \mathcal{A}_r$. For $c \geq 0$, we furthermore write $\mu \xrightarrow{c} \lambda$ if λ is obtained from μ by adding a skew column of c boxes and $\mu \xrightarrow{-c} \lambda$ if λ is obtained from μ by removing a skew column of c boxes. We often write $-c$ as \bar{c} .

The following is the fundamental combinatorial object considered in this paper.

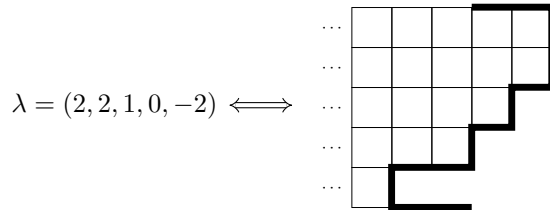


FIGURE 1. A generalized partition with $r = 5$ rows. The right border has been drawn in bold.

Definition 2.1. An r -row *skew fluctuating tableau* of length n is a sequence

$$T = \lambda^0 \xrightarrow{c_1} \lambda^1 \xrightarrow{c_2} \dots \xrightarrow{c_n} \lambda^n$$

$$T = 0000 \xrightarrow{2} 1100 \xrightarrow{\bar{1}} 110\bar{1} \xrightarrow{3} 2110 \xrightarrow{1} 2210 \xrightarrow{\bar{2}} 2100 \xrightarrow{2} 2111 \xrightarrow{\bar{1}} 1111$$

	1	$3\bar{7}$
	1	$4\bar{5}$
	$3\bar{5}6$	
$\bar{2}3$	6	

FIGURE 2. The visualization of our running example fluctuating tableau T with 4 rows, length 7, shape $\mathbf{1} = (1, 1, 1, 1)$, and type $(2, \bar{1}, 3, 1, \bar{2}, 2, \bar{1})$. Cells in the (final) shape are in light grey. The thick line indicates the outline of the initial shape $\mathbf{0} = (0, 0, 0, 0)$.

of r -row generalized partitions such that λ^{i-1} and λ^i differ by a skew column obtained by adding c_i or removing $-c_i$ cells for all $1 \leq i \leq n$. The partition λ^0 is called the *initial shape* of T and λ^n is called the *final shape* of T . The sequence $\underline{c} = (c_1, \dots, c_n) \in \{0, \pm 1, \dots, \pm r\}^n$ is the *type* of T . When $\lambda^0 = (0, \dots, 0)$, we drop the adjective “skew” and refer to the final shape as simply the *shape*. Let $\text{FT}(r, n, \mu, \lambda, \underline{c})$ be the set of skew fluctuating tableaux with r rows, length n , initial shape μ , final shape λ , and type \underline{c} . We will drop some parameters from $\text{FT}(r, n, \mu, \lambda, \underline{c})$ as convenient.

Building on work of Patrias [Pat19], we visualize fluctuating tableaux by writing i in the added cells of $\lambda^i - \lambda^{i-1}$ or \bar{i} in the removed cells of $\lambda^{i-1} - \lambda^i$; see Figure 2 for an example. We indicate the outline of the initial shape with a bold line as in Figure 1.

Our main applications of fluctuating tableaux involve the natural fluctuating analogue of rectangular standard tableaux.

Definition 2.2. A fluctuating tableau is *rectangular* if its shape λ is a *generalized rectangle*, meaning $\lambda_1 = \dots = \lambda_r$. We say a fluctuating tableau of type (c_1, \dots, c_n) is of *oscillating type* if each $c_j \in \{\pm 1\}$.

Remark 2.3. Fluctuating tableaux whose type consists of non-negative integers are *row-strict* or “transpose semistandard” tableaux. Standard tableaux are fluctuating tableaux of type $(1, \dots, 1)$. In the context of semistandard tableaux, “type” is often referred to as “content.”

Fluctuating tableaux of oscillating type are referred to as *up-down staircase tableaux* in [Ste87] and as *generalized oscillating tableaux* in [Pat19]. We use the terminology from [Pat19], but drop the word ‘generalized’ for brevity. In [PP21], the rectangular $r = 3$ cases with type consisting of 1’s and 2’s are called *Russell tableaux* after [Rus13]. Allowing skew columns to be added or removed is essential our work in [GPPSS23a] on applications of fluctuating tableaux to webs and the representation category of SL_4 .

2.2. Fluctuating tableaux and $\text{GL}_r(\mathbb{C})$ representation theory. The irreducible rational representations of $\text{GL}_r(\mathbb{C})$ are naturally indexed by r -row generalized partitions (see, e.g., [Ste87, §2]). Write $V(\lambda)$ for the irreducible associated to λ . Consider the tuples $\omega_i = (1^i, 0^{r-i})$ and $\bar{\omega}_i = \omega_{\bar{i}} = (0^{r-i}, \bar{1}^i)$, which correspond to adding or removing a column of size i . These tuples also correspond to exterior powers,

$$V(\omega_i) \cong \bigwedge^i V \quad \text{and} \quad V(\bar{\omega}_i) \cong \bigwedge^i V^* \quad (0 \leq i \leq r),$$

where $V \cong \mathbb{C}^r$ is the defining representation and V^* is the dual of V . In particular, $V(\mathbf{1}) \cong \det$ and $V(\bar{\mathbf{1}}) \cong \det^* \cong 1/\det$. As a shorthand, we write $\bigwedge^{-i} V := \bigwedge^i V^*$.

Given a type $\underline{c} = (c_1, \dots, c_n)$, let

$$(2.1) \quad \bigwedge^{\underline{c}} V = \bigwedge^{c_1} V \otimes \cdots \otimes \bigwedge^{c_n} V.$$

The dual Pieri rule gives the following. A crystal-theoretic proof is described in Section 8.3.

Theorem 2.4. *The multiplicity of the irreducible representation $V(\lambda)$ in $\bigwedge^{\underline{c}} V$ is the number of fluctuating tableaux of shape λ and type \underline{c} .*

Example 2.5. Recall that $V \otimes V^*$ may be identified with the set of $r \times r$ matrices. Thus $\bigwedge^{(1, -1)} V$ is the adjoint representation of $\mathrm{GL}_r(\mathbb{C})$. When $\underline{c} = (1, -1, 1, -1, \dots, 1, -1)$ has length $2k$, $\bigwedge^{\underline{c}} V$ is the k th tensor power of the adjoint representation. Stembridge [Ste87, §4] refers to the corresponding fluctuating tableaux as *alternating tableaux*, since they alternately add and remove single cells. The $\mathrm{GL}_r(\mathbb{C})$ -irreducible decomposition of $(V \otimes V^*)^{\otimes k}$ may be computed by enumerating all alternating tableaux of length $2k$ according to their final shape.

Let \mathfrak{S}_n denote the symmetric group of permutations of $[n] := \{1, \dots, n\}$. The factors in the tensor products $\bigwedge^{\underline{c}} V$ may be permuted without changing the isomorphism type. Consequently, we have the following symmetry in fluctuating tableaux.

Corollary 2.6. *For any permutation $\sigma \in \mathfrak{S}_n$,*

$$\# \mathrm{FT}(r, n, \lambda, (c_1, \dots, c_n)) = \# \mathrm{FT}(r, n, \lambda, (c_{\sigma_1}, \dots, c_{\sigma_n})).$$

We give a direct combinatorial proof of Corollary 2.6 in Section 4.1 by defining Bender–Knuth involutions on (skew) fluctuating tableaux. A crystal-theoretic argument is discussed in Section 8.3.

It is well-known that the representations $\bigwedge^{\underline{c}} V$ contain all of the irreducible rational representations $V(\lambda)$ of $\mathrm{GL}_r(\mathbb{C})$. For many purposes, one may study the $\bigwedge^{\underline{c}} V$ instead of the $V(\lambda)$. To make this statement precise, we first need an additional definition.

Definition 2.7. The *extremal fluctuating tableau* of type \underline{c} is the unique fluctuating tableau obtained by starting at \emptyset and successively adding top-justified columns of size c_i if $c_i \geq 0$ or removing bottom-justified columns of size $-c_i$ if $c_i \leq 0$.

Example 2.8. The extremal fluctuating tableau of type $(2, \bar{1}, 3, 2, \bar{2}, 2, \bar{1})$ has shape $(4, 4, 0, \bar{3})$:

				1	3	4	6
				1	3	4	6
				3	$\bar{5}$		
$\bar{7}$	$\bar{5}$	$\bar{2}$					

The shape of the extremal fluctuating tableau of type \underline{c} is the generalized partition

$$\omega_{\underline{c}} = \sum_{i=1}^n \omega_{c_i}.$$

Moreover, every generalized partition is of the form $\omega_{\underline{c}}$ for some \underline{c} . Define *lexicographic order* on tuples of integers by $\underline{c} <_{\mathrm{lex}} \underline{d}$ if the leftmost nonzero entry of $\underline{d} - \underline{c}$ is positive. It is straightforward to see that the extremal fluctuating tableau of type \underline{c} is the unique fluctuating tableau of type \underline{c} and shape $\omega_{\underline{c}}$, and that all other fluctuating tableaux of type \underline{c} have smaller final shape. In particular, we have the following.

Proposition 2.9. *There is a unique copy of $V(\omega_{\underline{c}})$ in $\bigwedge^{\underline{c}} V$. Each other $V(\lambda)$ in $\bigwedge^{\underline{c}} V$ has $\lambda <_{\mathrm{lex}} \omega_{\underline{c}}$.*

2.3. Fluctuating tableaux and $\mathrm{SL}_r(\mathbb{C})$ representation theory. We now summarize the role of fluctuating tableaux in the representation theory of $\mathrm{SL}_r(\mathbb{C})$. The rational representations are the same as for $\mathrm{GL}_r(\mathbb{C})$, except that $\det \cong 1$, and more generally $V(\lambda) \cong V(\mu)$ if and only if $\lambda = \mu + c \cdot \mathbf{1}$ for some $c \in \mathbb{Z}$. Consequently, we say the *weight* of a fluctuating tableau is the image of the shape in the quotient $\mathbb{Z}^r / \mathbb{Z}$. Note that the weight $\mathbf{0}$ fluctuating tableaux are precisely the rectangular fluctuating tableaux.

Let $\mathrm{Inv}_{\mathrm{SL}_r}(W)$ denote the subspace of SL_r -invariant elements of the representation W . Equivalently, this is the isotypic component of W with trivial SL_r -action. By Theorem 2.4 and the preceding paragraph, we have the following.

Proposition 2.10. *The r -row rectangular fluctuating tableaux of type \underline{c} index a basis of*

$$\mathrm{Inv}_{\mathrm{SL}_r}(\bigwedge^{\underline{c}} V).$$

In particular, rectangular fluctuating tableaux with r rows and type (1^n) are precisely $r \times (n/r)$ rectangular standard tableaux, which index a basis for $\mathrm{Inv}_{\mathrm{SL}_r}(V^{\otimes n})$. This invariant space may also be identified with the homogeneous coordinate ring of a Grassmannian with respect to its Plücker embedding.

2.4. Lattice words. Recall \mathcal{A}_r is the alphabet consisting of subsets of $\{\pm 1, \dots, \pm r\}$ whose elements are all of the same sign. The *lattice word* associated to a skew fluctuating tableau $T \in \mathrm{FT}(r, n)$ is the word $L = L(T) = w_1 \dots w_n$ in \mathcal{A}_r , where $\lambda^i = \lambda^{i-1} + \mathbf{e}_{w_i}$. We may recover T from $L(T)$ and the initial shape λ^0 , so in the non-skew case we sometimes identify T and $L(T)$. In our running example of Figure 2, $L(T) = \{12\}\bar{4}\{134\}2\{\bar{3}\bar{2}\}\{34\}\bar{1}$. Here we have suppressed commas between elements and we have suppressed the curly braces for singletons.

A word w is a lattice word of a (non-skew) fluctuating tableau if and only if for every prefix $w_1 \dots w_k$ and every $1 \leq a \leq b \leq r$, we have

$$(2.2) \quad (\mathbf{e}_{w_1} + \dots + \mathbf{e}_{w_k})_a \geq (\mathbf{e}_{w_1} + \dots + \mathbf{e}_{w_k})_b.$$

More concretely, in each prefix we require the number of a 's minus the number of \bar{a} 's to be weakly greater than the number of b 's minus the number of \bar{b} 's. A fluctuating tableau is rectangular if and only if equality holds in (2.2) for all a, b with $k = n$; in this case, we call L *balanced*.

2.5. Three fundamental involutions. We now define three fundamental involutions on fluctuating tableaux. They are responsible for a pervasive 4-fold symmetry in many constructions. For example, the 14 growth rules of Khovanov–Kuperberg [KK99] in fact may be grouped into six orbits under these symmetries, with five of size 2 and one of size 4. See [RSSW01, §3] for a closely related 4-fold symmetry.

Definition 2.11. For any tuple $\alpha = (\alpha_1, \dots, \alpha_r)$, set $\mathrm{rev}(\alpha) := (\alpha_r, \dots, \alpha_1)$. Let

$$\begin{aligned} \tau \left(\mu \xrightarrow{c} \lambda \right) &:= \lambda \xrightarrow{\bar{c}} \mu \\ \varpi \left(\mu \xrightarrow{c} \lambda \right) &:= \mathrm{rev}(-\mu) \xrightarrow{\bar{c}} \mathrm{rev}(-\lambda) \\ \varepsilon \left(\mu \xrightarrow{c} \lambda \right) &:= \mathrm{rev}(-\lambda) \xrightarrow{c} \mathrm{rev}(-\mu). \end{aligned}$$

We call τ *time reversal*. Our notation for ϖ is inspired by the natural involution ω on symmetric functions that exchanges elementary and complete homogeneous symmetric functions; ϖ corresponds to dualization on the level of rational $\mathrm{GL}_r(\mathbb{C})$ -representations. We will later relate ε to evacuation on rectangular tableaux. The following properties are clear.

Lemma 2.12. *The operators $\tau, \varpi, \varepsilon$ satisfy*

- ♦ $\tau^2 = \varpi^2 = \varepsilon^2 = \mathrm{id}$;
- ♦ $\tau, \varpi, \varepsilon$ pairwise commute; and
- ♦ each is the composite of the other two.

That is, they form a representation of a Klein 4-group.

We extend the definitions of $\tau, \varpi, \varepsilon$ in the obvious way to apply to fluctuating tableau T , obtaining fluctuating tableaux $\tau(T), \varpi(T)$, and $\varepsilon(T)$. Note that the initial and final shapes of a fluctuating tableau are preserved by ϖ , but are swapped by τ and ε . However, if we subtract \mathbf{c} throughout to ensure the result begins with $\mathbf{0}$, then τ and ε send rectangular fluctuating tableaux with final shape \mathbf{c} to rectangular fluctuating tableaux with final shape $-\mathbf{c}$. Such constant shifts do not materially affect any of our arguments, so we do not mention them further.

The effects of $\tau, \varpi, \varepsilon$ on lattice words are as follows.

Definition 2.13. Consider a word $L = w_1 \dots w_n$ in the alphabet \mathcal{A}_r . Define

- (i) $\tau(L) = \overline{w_n} \dots \overline{w_1}$;
- (ii) $\varpi(L) = \varpi(w_1) \dots \varpi(w_n)$, where $\varpi(w)$ replaces each element i in w with $-\text{sgn}(i)(r - |i| + 1)$; and
- (iii) $\varepsilon(L) = \varepsilon(w_n) \dots \varepsilon(w_1)$, where $\varepsilon(w)$ replaces each element i in w with $\text{sgn}(i)(r - |i| + 1)$.

It is easy to see that

$$L(\tau(T)) = \tau(L(T)), \quad L(\varpi(T)) = \varpi(L(T)), \quad \text{and} \quad L(\varepsilon(T)) = \varepsilon(L(T)).$$

Example 2.14. Given the fluctuating tableau T in Figure 2, the lattice word

$$L(T) = \{12\}\overline{4}\{134\}2\{\overline{32}\}\{34\}\overline{1}.$$

We then have

$$\begin{aligned} \tau(L(T)) &= 1\{\overline{43}\}\{23\}\overline{2}\{\overline{431}\}4\{\overline{21}\}, \\ \varpi(L(T)) &= \{\overline{43}\}1\{\overline{421}\}\overline{3}\{23\}\{\overline{21}\}4, \text{ and} \\ \varepsilon(L(T)) &= \overline{4}\{12\}\{\overline{32}\}3\{124\}\overline{1}\{34\}. \end{aligned}$$

When T is rectangular, we declare the initial shape of $\tau(T)$ and $\varepsilon(T)$ to be $\mathbf{0}$, so the resulting rectangular fluctuating tableaux are precisely encoded by $\tau(L(T))$ and $\varepsilon(L(T))$.

2.6. Oscillization.

Definition 2.15. Consider $\mu \xrightarrow{c} \lambda$. Let $\lambda = \mu + \mathbf{e}_{\{i_1 < \dots < i_c\}}$. The *oscillization* of $\mu \xrightarrow{c} \lambda$ is the sequence

$$\text{osc}(\mu \xrightarrow{c} \lambda) := \mu \rightarrow \mu^1 \rightarrow \dots \rightarrow \mu^{|c|-1} \rightarrow \lambda,$$

where

$$\mu^j = \mu^{j-1} + \mathbf{e}_{i_j}$$

with $\mu^0 := \mu$ and $\mu^{|c|} = \lambda$.

Given a fluctuating tableau $T = \lambda^0 \rightarrow \lambda^1 \rightarrow \dots \rightarrow \lambda^n$, let $\text{osc}(T)$ be the concatenation of $\text{osc}(\lambda^{i-1} \rightarrow \lambda^i)$ for $1 \leq i \leq n$. A fluctuating tableau is in the image of oscillization if and only if it is of oscillating type. Oscillization may be described easily in terms of lattice words. To compute $L(\text{osc}(T))$, we simply erase the curly braces from $L(T)$, where elements of each letter are written in increasing order, keeping the same initial and final shape. In our running example from Figure 2, $\text{osc}(T) = 12\overline{4}13423\overline{2}34\overline{1}$. Compare Figure 2 to Figure 3 for a pictorial interpretation.

3. LOCAL RULES, PROMOTION, AND EVACUATION

There are many ways one may define promotion: via Bender–Knuth involutions, jeu de taquin, growth rules, or cactus group actions based on Lusztig’s involution. We show all of these definitions are equivalent for fluctuating tableaux. These equivalences are known to experts for the main special cases, such as for semistandard tableaux; such experts can probably safely skip this section and the next one, as the extension to fluctuating tableaux behaves mostly as expected.

$$\text{osc}(T) = \begin{array}{|c|c|} \hline 1 & 4\overline{12} \\ \hline 2 & 7\overline{9} \\ \hline 5\overline{8}10 & \\ \hline \overline{3}6 & 11 \\ \hline \end{array}$$

FIGURE 3. The oscillization of the fluctuating tableau T from Figure 2.

We begin in this section with the most combinatorially simple definition of promotion and evacuation using a direct description of local rules, borrowed from van Leeuwen [vL98]. In Section 4, we then define the corresponding Bender–Knuth involutions tableau-theoretically and describe jeu de taquin on fluctuating tableaux. We show there that all three combinatorial definitions of promotion are equivalent.

Our emphasis on local rule diagrams has many similarities with the approaches taken in special cases by Chmutov–Glick–Pylyavskyy [CGP20, §3] and Westbury [Wes18, §5-6], which in turn built on work of Lenart [Len08] and Henriques–Kamnitzer [HK06]; see also, [BPS16, §2] and [Pat19].

3.1. Local rules. Fomin’s *growth diagrams* (see, e.g., [Sta99, Appendix 1]) can be used to define promotion, evacuation, and jeu de taquin for (semi)standard tableaux. In [vL98, Rule 4.1.1], van Leeuwen introduced certain explicit *local rules* generalizing those used to construct Fomin’s growth diagrams. Here, we apply van Leeuwen’s construction in the context of fluctuating tableaux, where we allow both addition and removal of skew columns. The approach we take here is intended to be as combinatorially direct and self-contained as possible, with no reference to Littelman paths, dominant weights, etc.

Given a tuple $\alpha \in \mathbb{Z}^n$, let $\text{sort}(\alpha)$ denote the generalized partition that is the weakly decreasing rearrangement of α .

Definition 3.1. A *local rule diagram* is a square

$$(3.1) \quad \begin{array}{ccc} \lambda & \xrightarrow{d} & \nu \\ \uparrow c & & \uparrow c \\ \kappa & \xrightarrow{d} & \mu \end{array}$$

where

$$(3.2) \quad \mu = \text{sort}(\nu + \kappa - \lambda) \quad \text{and} \quad \lambda = \text{sort}(\nu + \kappa - \mu),$$

with pointwise addition and subtraction.

A *local rule* fills in a missing lower right or upper left corner in (3.1) with μ or λ as determined by (3.2). See Figure 4 for an application of local rules. We will shortly see that the two conditions of (3.2) imply each other, so local rules result in local rule diagrams.

In the standard case, the local rules are uniquely determined by the fact there are at most two ways to complete (3.1), since rank two intervals in Young’s lattice have either 1 or 2 intermediate elements. Given $\kappa \xrightarrow{1} \lambda \xrightarrow{1} \nu$, we have $\mu = \lambda$ in the first case and $\mu \neq \lambda$ in the second.

We may typically reduce to the semistandard case using the following operators, which are combinatorial shadows of the $\text{GL}_r(\mathbb{C})$ -isomorphisms $\bigwedge^c V \cong \bigwedge^{r-c} V^* \otimes \det$.

Definition 3.2. The *switch* involution is given by

$$\text{switch}(\mu \xrightarrow{c} \lambda) = \mu \xrightarrow{-\text{sgn}(c)(r-|c|)} \lambda - \text{sgn}(c)\mathbf{1}.$$

$$\begin{array}{ccc}
220\overline{11} & \xrightarrow{3} & 32000 \\
\uparrow 4 & & \uparrow 4 \\
11\overline{112} & \xrightarrow[3]{\text{sort}(20\overline{101}) = 210\overline{11}} &
\end{array}$$

FIGURE 4. An example of using a local rule to fill in the lower right corner of a local rule diagram. Here, note that $20\overline{101} = 32000 + 11\overline{112} - 220\overline{11}$.

Example 3.3. Consider $2210 \xrightarrow{2} 2100$. Applying **switch** gives $2210 \xrightarrow{2} 3211$. Note that **switch** has replaced taking away 2 boxes with instead adding the complementary 2 boxes. Similarly, we have $\text{switch}(1100 \xrightarrow{1} 110\overline{1}) = 1100 \xrightarrow{3} 2210$.

Lemma 3.4. *Applying local rules results in local rule diagrams.*

Proof. Suppose $\kappa \xrightarrow{c} \lambda \xrightarrow{d} \nu$ is given and let $\mu = \text{sort}(\nu + \kappa - \lambda)$. We need to show that $\lambda = \text{sort}(\nu + \kappa - \mu)$.

Say $\lambda = \kappa + \mathbf{e}_S$ and $\nu = \lambda + \mathbf{e}_T$. Then $\nu + \kappa - \lambda = \kappa + \mathbf{e}_T$. Using **switch** operators, we may assume without loss of generality that $c, d \geq 0$ and $S, T \subset [r]$. Let $\Delta = (S \cup T) - (S \cap T)$ be the symmetric difference. Define an equivalence relation on Δ where $i \equiv j$ if and only if $\kappa_i = \kappa_j$. Since λ and ν are generalized partitions, the equivalence classes of Δ are of the form $\{i+1, \dots, i+a+b\}$, for some $a, b \in \mathbb{N}$, where $\{i+1, \dots, i+a\} \subseteq S$ and $\{i+a+1, \dots, i+a+b\} \subseteq T$.

Let U be the union of $S \cap T$ and intervals $\{i+1, \dots, i+b\}$ for each equivalence class of Δ , and let V be the union of $S \cap T$ and the intervals $\{i+b+1, \dots, i+b+a\}$, so that $\mathbf{e}_S + \mathbf{e}_T = \mathbf{e}_U + \mathbf{e}_V$. We now find that $\text{sort}(\kappa + \mathbf{e}_T) = \kappa + \mathbf{e}_U$ and $\text{sort}(\kappa + \mathbf{e}_V) = \kappa + \mathbf{e}_S$. Hence, $\mu = \text{sort}(\nu + \kappa - \lambda) = \text{sort}(\kappa + \mathbf{e}_T) = \kappa + \mathbf{e}_U$, $\nu = \mu + \mathbf{e}_V$, $\kappa \xrightarrow{d} \mu \xrightarrow{c} \nu$, and $\text{sort}(\nu + \kappa - \mu) = \text{sort}(\kappa + \mathbf{e}_V) = \kappa + \mathbf{e}_S = \lambda$. \square

The $\tau, \varpi, \varepsilon$ involutions of Definition 2.11 may also be applied to local rule diagrams.

Lemma 3.5. *Applying $\tau, \varpi, \varepsilon$ to local rule diagrams results in local rule diagrams:*

$$\begin{array}{ccc}
\begin{array}{ccc} \lambda & \xrightarrow{d} & \nu \\ c \uparrow & & \uparrow c \\ \kappa & \xrightarrow{d} & \mu \end{array} & \xleftrightarrow{\tau} & \begin{array}{ccc} \lambda & \xleftarrow{\bar{d}} & \nu \\ \bar{c} \downarrow & & \downarrow \bar{c} \\ \kappa & \xleftarrow{\bar{d}} & \mu \end{array} \\
& \searrow \varpi & \\
\begin{array}{ccc} \text{rev}(-\lambda) & \xleftarrow{d} & \text{rev}(-\nu) \\ c \downarrow & & \downarrow c \\ \text{rev}(-\kappa) & \xleftarrow{d} & \text{rev}(-\mu) \end{array} & \xleftrightarrow{\tau} & \begin{array}{ccc} \text{rev}(-\lambda) & \xrightarrow{\bar{d}} & \text{rev}(-\nu) \\ \bar{c} \uparrow & & \uparrow \bar{c} \\ \text{rev}(-\kappa) & \xrightarrow{\bar{d}} & \text{rev}(-\mu) \end{array} \\
& \uparrow \varepsilon & \\
& & \begin{array}{ccc} \mu & \xrightarrow{\bar{d}} & \kappa \\ \bar{c} \uparrow & & \uparrow \bar{c} \\ \nu & \xrightarrow{\bar{d}} & \lambda \end{array}
\end{array}$$

Proof. The result is clear for τ . For ϖ , it reduces to the fact that $\text{sort}(-\text{rev}(\alpha)) = \text{rev}(-\text{sort}(\alpha))$. Finally, by Lemma 2.12, ε is the composite of τ and ϖ . \square

For later use, it will be convenient to consistently orient growth diagrams with edges going north or east. Consequently when applying τ or ε , we rotate all diagrams by 180° :

$$\tau \left(\begin{array}{ccc} \lambda & \xrightarrow{d} & \nu \\ c \uparrow & & \uparrow c \\ \kappa & \xrightarrow{d} & \mu \end{array} \right) = \begin{array}{ccc} \mu & \xrightarrow{\bar{d}} & \kappa \\ \bar{c} \uparrow & & \uparrow \bar{c} \\ \nu & \xrightarrow{\bar{d}} & \lambda \end{array} \quad \text{and} \quad \varepsilon \left(\begin{array}{ccc} \lambda & \xrightarrow{d} & \nu \\ c \uparrow & & \uparrow c \\ \kappa & \xrightarrow{d} & \mu \end{array} \right) = \begin{array}{ccc} \text{rev}(-\mu) & \xrightarrow{d} & \text{rev}(-\kappa) \\ c \uparrow & & \uparrow c \\ \text{rev}(-\nu) & \xrightarrow{d} & \text{rev}(-\lambda) \end{array}$$

3.2. Promotion and evacuation diagrams. Given a skew fluctuating tableau, we use local rules to fill certain diagrams, allowing us to compute promotion, evacuation, and dual evacuation.

Definition 3.6. The *promotion diagram* of the skew fluctuating tableau

$$T = \lambda^0 \xrightarrow{c_1} \lambda^1 \xrightarrow{c_2} \dots \xrightarrow{c_n} \lambda^n$$

is obtained by applying the local rules to recursively fill the bottom row of the diagram

$$\mathcal{P}\text{-diagram}(T) := \begin{array}{c} \overbrace{\lambda^{00} \xrightarrow{c_1} \lambda^{01} \xrightarrow{c_2} \dots \xrightarrow{c_n} \lambda^{0n}}^T \\ \begin{array}{c} \parallel \uparrow c_1 \uparrow c_1 \uparrow c_1 \parallel \\ \lambda^{11} \xrightarrow{-c_2} \dots \xrightarrow{-c_n} \lambda^{1n} \xrightarrow{-c_1} \lambda^{1,n+1} \end{array} \\ \underbrace{\hspace{10em}}_{\mathcal{P}(T)} \end{array}$$

from left to right, subject to the boundary conditions

$$\lambda^{0i} = \lambda^i, \lambda^{11} = \lambda^0, \text{ and } \lambda^{1,n+1} = \lambda^n.$$

The *promotion* of T is the bottom row of $\mathcal{P}\text{-diagram}(T)$:

$$\mathcal{P}(T) := \lambda^{11} \xrightarrow{c_2} \dots \xrightarrow{c_n} \lambda^{1n} \xrightarrow{c_1} \lambda^{1,n+1}.$$

Definition 3.7. The *evacuation diagram* and *dual evacuation diagram* of the skew fluctuating tableau

$$T = \lambda^0 \xrightarrow{c_1} \lambda^1 \xrightarrow{c_2} \dots \xrightarrow{c_n} \lambda^n$$

are obtained by recursively applying local rules to fill the triangles

$$\begin{array}{cc} \mathcal{E}\text{-diagram}(T) = & \mathcal{E}^*\text{-diagram}(T) = \\ (3.3) \quad \begin{array}{c} \overbrace{\lambda^{00} \xrightarrow{c_1} \lambda^{01} \xrightarrow{c_2} \dots \xrightarrow{c_n} \lambda^{0n}}^T \\ \begin{array}{c} \parallel \uparrow c_1 \uparrow c_1 \uparrow c_1 \parallel \\ \lambda^{11} \xrightarrow{-c_2} \dots \xrightarrow{-c_n} \lambda^{1n} \\ \parallel \uparrow c_2 \uparrow c_2 \uparrow c_2 \parallel \\ \vdots \xrightarrow{-c_n} \vdots \\ \parallel \uparrow c_n \uparrow c_n \parallel \\ \lambda^{nn} \end{array} \end{array} & \begin{array}{c} \lambda^{-n,0} \\ \uparrow c_1 \parallel \\ \vdots \xrightarrow{-c_1} \vdots \\ \uparrow c_{n-1} \parallel \\ \lambda^{-1,0} \xrightarrow{-c_1} \dots \xrightarrow{-c_{n-1}} \lambda^{-1,n-1} \\ \uparrow c_n \parallel \\ \lambda^{00} \xrightarrow{c_1} \dots \xrightarrow{c_{n-1}} \lambda^{0,n-1} \xrightarrow{c_n} \lambda^{0,n} \\ \underbrace{\hspace{10em}}_T \end{array} \end{array}$$

from upper left to lower right for $\mathcal{E}\text{-diagram}(T)$ and from lower right to upper left for $\mathcal{E}^*\text{-diagram}(T)$, subject to the boundary conditions

$$\lambda^{0i} = \lambda^i, \lambda^{ii} = \lambda^0, \text{ and } \lambda^{i,n+i} = \lambda^n.$$

The *evacuation* of T is the right column of $\mathcal{E}\text{-diagram}(T)$:

$$\mathcal{E}(T) = \lambda^{nn} \xrightarrow{c_n} \dots \xrightarrow{c_2} \lambda^{1n} \xrightarrow{c_1} \lambda^{0n}.$$

Similarly, the *dual evacuation* of T is the left column of $\mathcal{E}^*\text{-diagram}(T)$:

$$\mathcal{E}^*(T) = \lambda^{00} \xrightarrow{c_n} \lambda^{-1,0} \xrightarrow{c_{n-1}} \dots \xrightarrow{c_1} \lambda^{-n,0}.$$

We combine promotion, evacuation, and dual evacuation diagrams in the following parallelogram.

Definition 3.8. The *promotion-evacuation diagram* of the skew fluctuating tableau

$$T = \lambda^0 \xrightarrow{c_1} \lambda^1 \xrightarrow{c_2} \dots \xrightarrow{c_n} \lambda^n$$

is obtained by recursively applying local rules to fill the parallelogram

$$(3.4) \quad \mathcal{PE}\text{-diagram}(T) :=$$

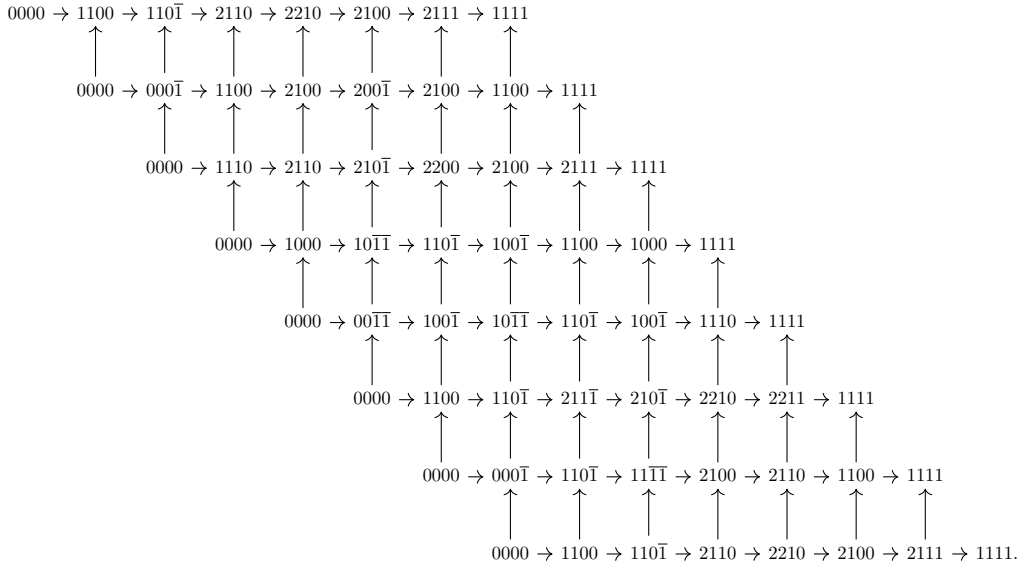
from upper left to lower right subject to the boundary conditions

$$\lambda^{0i} = \lambda^i, \lambda^{ii} = \lambda^0, \text{ and } \lambda^{i,n+i} = \lambda^n.$$

Note that the i th power of promotion of T is the i th row of $\mathcal{PE}\text{-diagram}(T)$, indexing from 0 at the top. In particular, the bottom row of $\mathcal{PE}\text{-diagram}(T)$ is $\mathcal{P}^n(T)$. The promotion-evacuation diagram is the concatenation of evacuation and dual evacuation diagrams:

$$(3.5) \quad \mathcal{PE}\text{-diagram}(T) = \mathcal{E}\text{-diagram}(T) \parallel \mathcal{E}^*\text{-diagram}(\mathcal{P}^n(T)).$$

Example 3.9. For the fluctuating tableau T of Figure 2, $\mathcal{PE}\text{-diagram}(T)$ is



In particular,

$$\begin{aligned} T &= 0000 \rightarrow 1100 \rightarrow 1101\bar{} \rightarrow 2110 \rightarrow 2210 \rightarrow 2100 \rightarrow 2111 \rightarrow 1111, \\ \mathcal{P}(T) &= 0000 \rightarrow 000\bar{} \rightarrow 1100 \rightarrow 2100 \rightarrow 200\bar{} \rightarrow 2100 \rightarrow 1100 \rightarrow 1111, \\ \mathcal{E}(T) &= 0000 \rightarrow 000\bar{} \rightarrow 110\bar{} \rightarrow 10\bar{} \rightarrow 100\bar{} \rightarrow 2100 \rightarrow 1100 \rightarrow 1111, \text{ and} \\ \mathcal{E}^*(T) &= \mathcal{E}(T). \end{aligned}$$

In terms of lattice words,

$$\begin{aligned} L(T) &= \{12\}\bar{4}\{134\}2\{\bar{32}\}\{34\}\bar{1}, \\ L(\mathcal{P}(T)) &= \bar{4}\{124\}1\{\bar{42}\}\{24\}\bar{1}\{34\}, \text{ and} \\ L(\mathcal{E}(T)) &= \bar{4}\{12\}\{\bar{32}\}3\{124\}\bar{1}\{34\} \\ &= L(\mathcal{E}^*(T)). \end{aligned}$$

In this particular case, $\mathcal{P}^n(T) = T$, $\mathcal{E}(T) = \mathcal{E}^*(T)$, and $L(\mathcal{E}(T)) = \varepsilon(L(T))$. As we will see, these properties are equivalent in general and moreover always hold when T is rectangular.

We will refer to promotion diagrams, evacuation diagrams, promotion-evacuation diagrams, etc., as *growth diagrams*.

Remark 3.10. The literature is inconsistent regarding the definition of “promotion.” If we replace $\mathcal{P}\text{-diagram}(T)$ with the dual notion as in $\mathcal{E}^*\text{-diagram}(T)$, the corresponding dual version of promotion is \mathcal{P}^{-1} . Some sources hence use “promotion” to refer to \mathcal{P}^{-1} .

The following properties are straightforward to verify from the definitions and the symmetry of local rules.

Lemma 3.11. *As operators on fluctuating tableaux, we have the following.*

$$\begin{aligned} \tau \circ \mathcal{E}\text{-diagram} &= \mathcal{E}^*\text{-diagram} \circ \tau & \tau \circ \mathcal{E}^*\text{-diagram} &= \mathcal{E}\text{-diagram} \circ \tau \\ \varepsilon \circ \mathcal{E}\text{-diagram} &= \mathcal{E}^*\text{-diagram} \circ \varepsilon & \varepsilon \circ \mathcal{E}^*\text{-diagram} &= \mathcal{E}\text{-diagram} \circ \varepsilon \\ \varpi \circ \mathcal{E}\text{-diagram} &= \mathcal{E}\text{-diagram} \circ \varpi & \varpi \circ \mathcal{E}^*\text{-diagram} &= \mathcal{E}^*\text{-diagram} \circ \varpi \\ \tau \circ \mathcal{P}\text{-diagram} &= \mathcal{P}\text{-diagram} \circ \tau \circ \mathcal{P} & \tau \circ \mathcal{P}\mathcal{E}\text{-diagram} &= \mathcal{P}\mathcal{E}\text{-diagram} \circ \varepsilon \circ \mathcal{E}^* \circ \tau \\ \varepsilon \circ \mathcal{P}\text{-diagram} &= \mathcal{P}\text{-diagram} \circ \varepsilon \circ \mathcal{P} & \varepsilon \circ \mathcal{P}\mathcal{E}\text{-diagram} &= \mathcal{P}\mathcal{E}\text{-diagram} \circ \varepsilon \circ \mathcal{E}^* \circ \varepsilon \\ \varpi \circ \mathcal{P}\text{-diagram} &= \mathcal{P}\text{-diagram} \circ \varpi & \varpi \circ \mathcal{P}\mathcal{E}\text{-diagram} &= \mathcal{P}\mathcal{E}\text{-diagram} \circ \varpi \end{aligned}$$

For standard tableaux, the following is [Sta09, Theorem 2.1]. The proof for fluctuating tableaux is essentially the same and we omit it.

Lemma 3.12. *On length n skew fluctuating tableaux, we have the following:*

- (i) \mathcal{P} is invertible;
- (ii) $\mathcal{E} \circ \mathcal{E} = \text{id}$, $\mathcal{E}^* \circ \mathcal{E}^* = \text{id}$;
- (iii) $\mathcal{E}^* \circ \mathcal{E} = \mathcal{P}^n$, $\mathcal{E} \circ \mathcal{E}^* = \mathcal{P}^{-n}$; and
- (iv) $\mathcal{P} \circ \mathcal{E} = \mathcal{E} \circ \mathcal{P}^{-1}$, $\mathcal{P} \circ \mathcal{E}^* = \mathcal{E}^* \circ \mathcal{P}^{-1}$.

In particular, \mathcal{P} and \mathcal{E} give a representation of the infinite dihedral group, as do \mathcal{P} and \mathcal{E}^* .

We also record the following consequence of Lemma 3.11.

Lemma 3.13. *On skew fluctuating tableaux, we have the following:*

- (i) ϖ commutes with each of \mathcal{P} , \mathcal{E} , and \mathcal{E}^* ;
- (ii) $\tau \circ \mathcal{P} = \mathcal{P}^{-1} \circ \tau$ and $\tau \circ \mathcal{E} = \mathcal{E}^* \circ \tau$;
- (iii) $\varepsilon \circ \mathcal{P} = \mathcal{P}^{-1} \circ \varepsilon$ and $\varepsilon \circ \mathcal{E} = \mathcal{E}^* \circ \varepsilon$.

Finally, the following lemma will be useful to us in studying rectangular fluctuating tableaux.

Lemma 3.14. *Let T be a length n skew fluctuating tableaux. The following are equivalent:*

- (i) $\mathcal{E}(T) = \varepsilon(T)$,
- (ii) $\mathcal{E}^*(T) = \varepsilon(T)$.

Moreover, they imply the following, which are also equivalent:

- (a) $\mathcal{E}(T) = \mathcal{E}^*(T)$,

(b) $\mathcal{P}^n(T) = T$.

Proof. The equivalence of (i) and (ii) follows from $\varepsilon \circ \mathcal{E} = \mathcal{E}^* \circ \varepsilon$ and the fact that all three of these operations are involutions (see Lemmas 2.12 and 3.12). Clearly (i) and (ii) imply (a). The equivalence of (a) and (b) follows from $\mathcal{E}^* \circ \mathcal{E} = \mathcal{P}^n$ (see Lemma 3.12). \square

4. BENDER–KNUTH INVOLUTIONS AND JEU DE TAQUIN

Our next goal is to encode the local rules in combinatorial manipulations on fluctuating tableaux. In Section 5, we will use this description via jeu de taquin to define the main new objects of interest in this paper, *promotion matrices* and *promotion permutations*.

4.1. Bender–Knuth involutions via local rules. Here we introduce Bender–Knuth involutions for fluctuating tableaux in terms of local rules and give their basic properties. For the case of semistandard tableaux, these involutions were first given in [BK72].

Definition 4.1. For $1 \leq i \leq n-1$, the i th *Bender–Knuth involution* BK_i on skew fluctuating tableaux is given by

$$\begin{aligned} \text{BK}_i(\lambda^0 \rightarrow \dots \rightarrow \lambda^{i-1} \rightarrow \lambda^i \rightarrow \lambda^{i+1} \rightarrow \dots \rightarrow \lambda^n) \\ = \lambda^0 \rightarrow \dots \rightarrow \lambda^{i-1} \rightarrow \mu^i \rightarrow \lambda^{i+1} \rightarrow \dots \rightarrow \lambda^n, \end{aligned}$$

where $\mu^i = \text{sort}(\lambda^{i+1} + \lambda^{i-1} - \lambda^i)$. Pictorially, we have

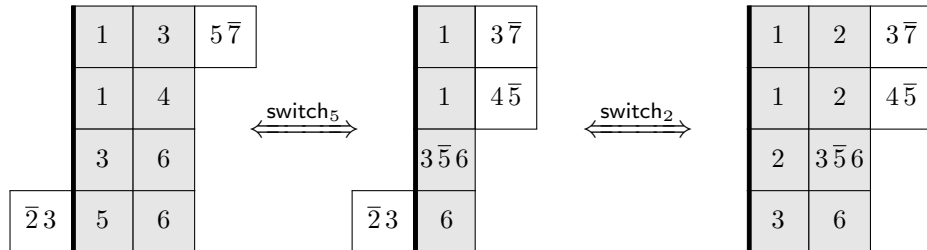
$$(4.1) \quad \begin{array}{ccccccc} & & & & \lambda^i & & \\ & & & \nearrow c_i & \parallel \text{BK}_i & \searrow c_{i+1} & \\ \lambda^0 & \xrightarrow{c_1} & \dots & \xrightarrow{c_{i-1}} & \lambda^{i-1} & & \lambda^{i+1} \xrightarrow{c_{i+2}} \dots \xrightarrow{c_n} \lambda^n \\ & & & \searrow c_{i+1} & \parallel & \nearrow c_i & \\ & & & & \mu^i & & \end{array}$$

We also extend the *switch* operator to skew fluctuating tableaux which toggle signs in the type of fluctuating tableaux.

Definition 4.2. Given a skew fluctuating tableau of length n and $1 \leq i \leq n$, define $\text{switch}_i(T)$ by replacing the i th step with its *switch*:

$$\begin{aligned} \text{switch}_i(\lambda^0 \xrightarrow{c_1} \dots \xrightarrow{c_{i-1}} \lambda^{i-1} \xrightarrow{c_i} \lambda^i \xrightarrow{c_{i+1}} \lambda^{i+1} \xrightarrow{c_{i+2}} \dots \xrightarrow{c_n} \lambda^n) \\ = \lambda^0 \xrightarrow{c_1} \dots \xrightarrow{c_{i-1}} \lambda^{i-1} \xrightarrow{\overline{r-c_i}} \lambda^i - \text{sgn}(c_i)\mathbf{1} \xrightarrow{c_{i+1}} \lambda^{i+1} - \text{sgn}(c_i)\mathbf{1} \xrightarrow{c_{i+2}} \dots \xrightarrow{c_n} \lambda^n - \text{sgn}(c_i)\mathbf{1}. \end{aligned}$$

Example 4.3. The fluctuating tableau T of Figure 2 is shown below, center. In Example 3.3, we computed the local action of switch_5 and switch_2 . Pictorially, we have



See also Figure 5 for further examples.

The following are direct consequences of the definitions and the symmetry of local rule diagrams. All of the proofs are similar and straightforward, so we mostly omit them.

Lemma 4.4. *On skew fluctuating tableaux of length n , BK_i and switch_j are involutions for which*

$$(4.2) \quad BK_i \circ \text{switch}_i = \text{switch}_{i+1} \circ BK_i \quad (1 \leq i \leq n-1).$$

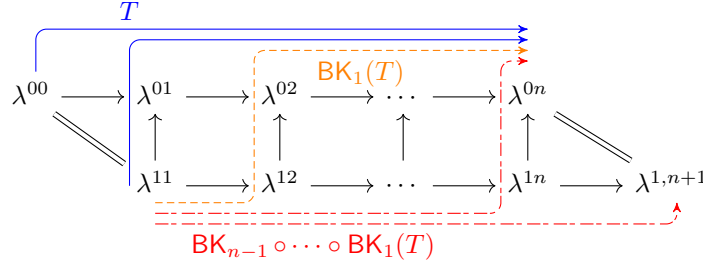
Moreover,

- (i) $BK_i \circ BK_j = BK_j \circ BK_i$ if $|i - j| > 1$
- (ii) $BK_i \circ \text{switch}_j = \text{switch}_j \circ BK_i$ for all $1 \leq i \leq n-1$, $1 \leq j \leq n$ with $j \neq i, i+1$
- (iii) $\text{switch}_i \circ \text{switch}_j = \text{switch}_j \circ \text{switch}_i$ if $i \neq j$.

Lemma 4.5. *On length n fluctuating tableaux, we have:*

- (i) $\mathcal{P} = BK_{n-1} \circ \cdots \circ BK_1$
- (ii) $\mathcal{E} = BK_1 \circ (BK_2 \circ BK_1) \circ \cdots \circ (BK_{n-1} \circ \cdots \circ BK_1)$
- (iii) $\mathcal{E}^* = (BK_{n-1} \circ \cdots \circ BK_1) \circ \cdots \circ (BK_{n-1} \circ BK_{n-2}) \circ BK_{n-1}$

Proof. The following diagram shows (i), by successively applying the Bender-Knuth involutions to the fluctuating tableau T , producing the promotion diagram of T .



For a similar perspective on these diagrams, see [Spe14, §6]. □

Lemma 4.6. *On length n fluctuating tableaux with r rows, we have:*

- (i) For $1 \leq i \leq n-1$,

$$\begin{aligned} BK_i \circ \varpi &= \varpi \circ BK_i, \\ BK_i \circ \tau &= \tau \circ BK_{n-i}, \text{ and} \\ BK_i \circ \varepsilon &= \varepsilon \circ BK_{n-i}. \end{aligned}$$

- (ii) For $1 \leq i \leq n$,

$$\begin{aligned} \text{switch}_i \circ \varpi &= \varpi \circ \text{switch}_i, \\ \text{switch}_i \circ \tau &= \tau \circ \text{switch}_{n+1-i} + \text{sgn}(c_{n+1-i})\mathbf{1}, \text{ and} \\ \text{switch}_i \circ \varepsilon &= \varepsilon \circ \text{switch}_{n+1-i} + \text{sgn}(c_{n+1-i})\mathbf{1}. \end{aligned}$$

- (iii) When i is taken modulo n ,

$$\begin{aligned} \text{switch}_i \circ \mathcal{P} &= \mathcal{P} \circ \text{switch}_{i+1}, \\ \text{switch}_i \circ \mathcal{E} &= \mathcal{E} \circ \text{switch}_{n+1-i}, \text{ and} \\ \text{switch}_i \circ \mathcal{E}^* &= \mathcal{E}^* \circ \text{switch}_{n+1-i}. \end{aligned}$$

4.2. Bender–Knuth involutions via tableaux. We next give a more direct, tableaux-theoretic description of BK_i . We broadly follow Stembridge’s account of the classical Bender–Knuth involutions on semistandard tableaux [Ste02], extended to fluctuating tableaux. See Figure 5 and Example 4.10 for examples.

Definition 4.7. Let $T \in \text{FT}(n, \underline{c})$ and fix $1 \leq i \leq n-1$. We call certain cells *free*, *forced*, *moving*, or *open* as follows.

- ♦ If $c_i \cdot c_{i+1} \geq 0$, call a cell *free* if it contains exactly one of $i, i+1, \bar{i}$, or $\overline{i+1}$ and no other cell in b 's row contains any of $i, i+1, \bar{i}$, or $\overline{i+1}$.
- ♦ If $c_i \cdot c_{i+1} \leq 0$, call cells containing exactly one of $i, i+1, \bar{i}$, or $\overline{i+1}$ *forced*. Call a cell *moving* if it contains both i and $\overline{i+1}$ or both \bar{i} and $i+1$. Additionally, for each row R which does not contain any of $i, i+1, \bar{i}$, or $\overline{i+1}$, we identify a cell b_R in R and call it *open*. Let j be the largest absolute value of an entry in R less than i , if any exist.
 - If $c_i \geq 0$, let b_R be the cell immediately right of the cell containing j , or the cell containing \bar{j} , or if j does not exist then let b_R be the cell immediately right of the rightmost cell of the initial shape in R .
 - If $c_i \leq 0$, let b_R be the cell containing j , or the cell immediately left of the cell containing \bar{j} , or otherwise the rightmost cell of the initial shape in R .

See Figure 5 for some examples.

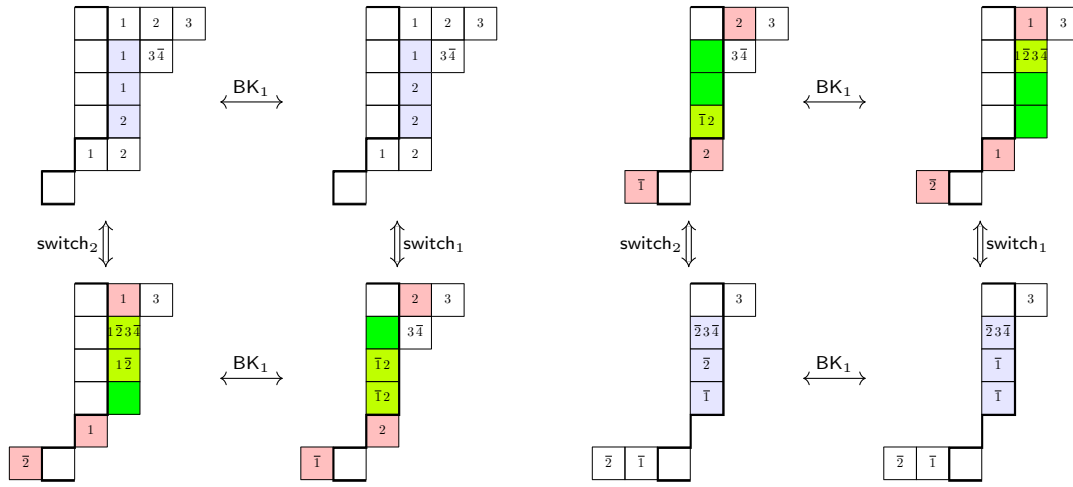


FIGURE 5. Interactions between the BK_i involutions and the $switch_j$ involutions. Free cells are highlighted in light blue \square . Forced cells are pink \blacksquare , moving cells are light green \blacksquare , and open cells are darker green \blacksquare .

Definition 4.8. For $1 \leq i \leq n-1$, the i th Bender–Knuth involution BK_i on skew fluctuating tableaux of length n is defined combinatorially as follows.

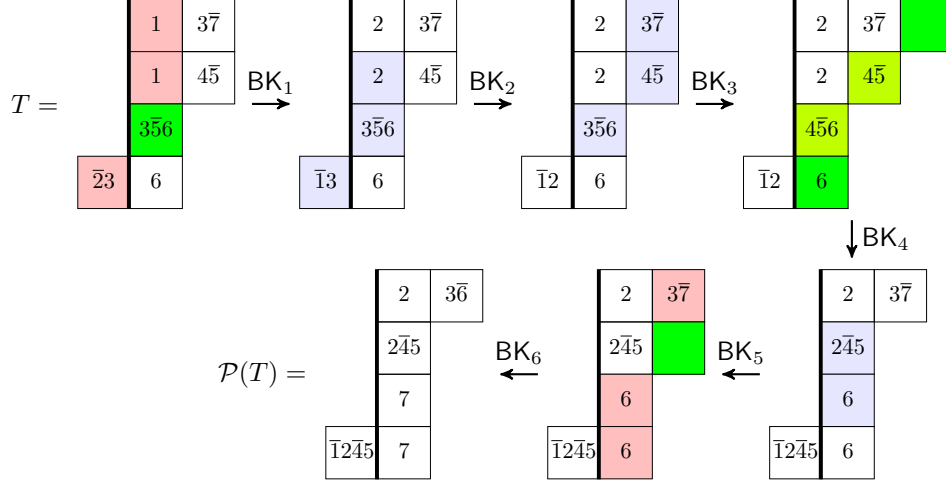
- ♦ If $c_i \cdot c_{i+1} \geq 0$, the free cells in each column form a connected segment, with a copies of i or $\bar{i+1}$ at the top and b copies of $i+1$ or \bar{i} at the bottom. Apply BK_i by replacing each such segment with b copies of i or $\bar{i+1}$ at the top and a copies of $i+1$ or \bar{i} at the bottom, leaving all other entries of T unchanged.
- ♦ If $c_i \cdot c_{i+1} \leq 0$, the collection of moving and open cells in each column forms a single connected segment.
 - If $c_i > 0$, such a segment has a moving cells above b open cells. In this case, apply BK_i by first moving all a copies of $i, \bar{i+1}$ from moving cells to the bottom a cells immediately left of the segment and then replacing these labels with $\bar{i}, i+1$.
 - If $c_i < 0$, such a segment has a open cells above b moving cells. In this case, apply BK_i by first moving all b copies of $\bar{i}, i+1$ from moving cells to the top b cells immediately right of the segment and then replacing these labels with $i, \bar{i+1}$.

Finally, in each forced cell, replace i with $i + 1$, $i + 1$ with i , \bar{i} with $\overline{i + 1}$, and $\overline{i + 1}$ with \bar{i} .

Lemma 4.9. *The combinatorial BK_i involutions are well-defined and agree with the local rule definition.*

Proof. When $c_i \cdot c_{i+1} \geq 0$, it is straightforward to see that the combinatorial description agrees with the local rule description in the proof of Lemma 3.4. When $c_i \cdot c_{i+1} \leq 0$, the combinatorial description agrees with that obtained by applying switch operators to the first case as in (4.2). \square

Example 4.10. Using the fluctuating tableau T from Figure 2, we compute $\mathcal{P}(T)$ with the following composite of Bender–Knuth involutions:



Here, we have used the same color-coding as in Figure 5.

4.3. oscillization and local rules. It is sometimes useful to oscillize growth diagrams. We begin by oscillizing local rules as follows. Recall $\text{osc}(\mu \xrightarrow{c} \lambda)$ from Definition 2.15.

Definition 4.11. The oscillization of the local rule diagram (3.1) is the diagram

$$(4.3) \quad \text{osc} \left(\begin{array}{ccc} \lambda & \xrightarrow{d} & \nu \\ c \uparrow & & \uparrow c \\ \kappa & \xrightarrow{d} & \mu \end{array} \right) := \begin{array}{ccccccc} \lambda & \longrightarrow & \lambda^1 & \longrightarrow & \dots & \longrightarrow & \lambda^{|d|-1} & \longrightarrow & \nu \\ \uparrow & & \uparrow & & \uparrow & & \uparrow & & \uparrow \\ \kappa^{|c|-1} & \longrightarrow & \cdot & \longrightarrow & \dots & \longrightarrow & \cdot & \longrightarrow & \nu^{|c|-1} \\ \uparrow & & \uparrow & & \uparrow & & \uparrow & & \uparrow \\ \vdots & \longrightarrow & \vdots & \longrightarrow & \ddots & \longrightarrow & \vdots & \longrightarrow & \vdots \\ \uparrow & & \uparrow & & \uparrow & & \uparrow & & \uparrow \\ \kappa^1 & \longrightarrow & \cdot & \longrightarrow & \dots & \longrightarrow & \cdot & \longrightarrow & \nu^1 \\ \uparrow & & \uparrow & & \uparrow & & \uparrow & & \uparrow \\ \kappa & \longrightarrow & \mu^1 & \longrightarrow & \dots & \longrightarrow & \mu^{|d|-1} & \longrightarrow & \mu \end{array}$$

where the edges on the boundary of the large rectangle are $\text{osc}(\kappa \xrightarrow{d} \mu)$, $\text{osc}(\lambda \xrightarrow{d} \nu)$, $\text{osc}(\kappa \xrightarrow{c} \lambda)$, and $\text{osc}(\mu \xrightarrow{c} \nu)$ and the cells are filled using local rules.

Note that we may fill the right-hand side of (4.3) from the upper left or from the lower right, or some mixture of the two. Every edge in the right-hand side of (4.3) either adds or removes a single cell.

In Lemma 4.13 we show the oscillization of a local rule diagram is well-defined. The proof uses the following lemma.

Lemma 4.12. *Consider the following refinement of the local rule diagram (3.1):*

$$(4.4) \quad \begin{array}{ccccc} \lambda & \xrightarrow{d_1} & \beta & \xrightarrow{d_2} & \nu \\ \uparrow c & & \uparrow c & & \uparrow c \\ \kappa & \xrightarrow{d_1} & \alpha & \xrightarrow{d_2} & \mu \end{array}$$

Here, $\kappa \xrightarrow{d_1} \alpha \xrightarrow{d_2} \mu$ and $\lambda \xrightarrow{d_1} \beta \xrightarrow{d_2} \nu$ have been obtained from $\text{osc}(\kappa \xrightarrow{d} \mu)$ and $\text{osc}(\lambda \xrightarrow{d} \nu)$ by collapsing edges. Then both squares in (4.4) are local rule diagrams.

Proof. Let $T = \kappa \xrightarrow{c} \lambda \xrightarrow{d} \nu$ and $S = \text{BK}_1(T) = \kappa \xrightarrow{d} \mu \xrightarrow{c} \nu$. Further let $T' = \kappa \xrightarrow{c} \lambda \xrightarrow{d_1} \beta \xrightarrow{d_2} \nu$ and $S' = \kappa \xrightarrow{d_1} \alpha \xrightarrow{d_2} \mu \xrightarrow{c} \nu$. The lemma follows from showing that $S' = \text{BK}_2 \circ \text{BK}_1(T')$. This may be verified directly from the combinatorial description of the Bender–Knuth involutions. Using **switch** involutions as necessary, we may reduce to the case that $c, d \geq 0$ and the free cells of T form a single column with c copies of 1 above d copies of 2. Then, T' has c copies of 1 above d_1 copies of 2 above d_2 copies of 3, so that $\text{BK}_2 \circ \text{BK}_1(T')$ has d_1 copies of 1 above d_2 copies of 2 above c copies of 3. On the other hand, S has d copies of 1 above c copies of 2, so S' also has d_1 copies of 1 above d_2 copies of 2 above c copies of 3. \square

Lemma 4.13. *The oscillization of a local rule diagram is well-defined.*

Proof. Filling the right-hand side of (4.3) results in an upper-left-justified collection A of squares and a lower-right-justified collection B of squares that meet along a path traveling by north and east steps from the lower-left corner to the upper-right corner. We must show A and B agree on this path. By extending A to the full $|c| \times |d|$ rectangle and using symmetry of local rules, it suffices to take $B = \emptyset$. That is, given the boundary edges $\text{osc}(\kappa \rightarrow \lambda)$ and $\text{osc}(\lambda \rightarrow \nu)$, we must show the remaining edges are $\text{osc}(\kappa \rightarrow \mu)$ and $\text{osc}(\mu \rightarrow \nu)$. We may now induct on $|c|, |d|$ by Lemma 4.12. The base case $|c| = |d| = 1$ is the fundamental symmetry from Lemma 3.4. \square

Definition 4.14. Let

$$(4.5) \quad \text{osc} \left(\begin{array}{ccc} \lambda & \xrightarrow{d} & \nu \\ & \uparrow d & \\ & \lambda & \end{array} \right) := \mathcal{E}\text{-diagram}(\text{osc}(\lambda \xrightarrow{d} \nu))$$

and

$$(4.6) \quad \text{osc} \left(\begin{array}{ccc} & \lambda & \\ c \uparrow & & \\ \kappa & \xrightarrow{c} & \lambda \end{array} \right) := \mathcal{E}^*\text{-diagram}(\text{osc}(\kappa \xrightarrow{c} \lambda)).$$

Definition 4.15. Let $\text{osc}(\mathcal{P}\text{-diagram}(T))$, $\text{osc}(\mathcal{E}\text{-diagram}(T))$, $\text{osc}(\mathcal{E}^*\text{-diagram}(T))$, and $\text{osc}(\mathcal{PE}\text{-diagram}(T))$ be obtained by oscillizing each component.

The lemma below follows by Lemma 4.13.

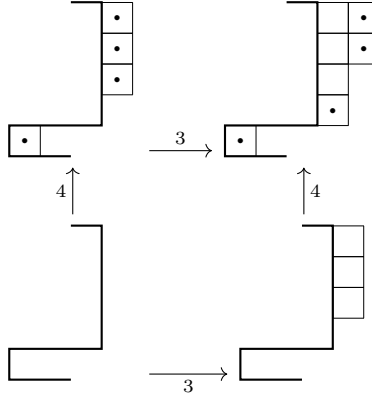
Lemma 4.16. *The operation osc commutes with \mathcal{P} -diagram, \mathcal{E} -diagram, \mathcal{E}^* -diagram, and \mathcal{PE} -diagram.*

4.4. **Jeu de taquin.** In a local rule diagram

$$\begin{array}{ccc} \lambda & \xrightarrow{d} & \nu \\ \uparrow c & & \uparrow c \\ \kappa & \xrightarrow{d} & \mu \end{array}$$

we may mark the $|c|$ added or removed cells in the fluctuating tableaux $\kappa \xrightarrow{c} \lambda$ and $\mu \xrightarrow{c} \nu$ with \bullet 's if $c \geq 0$ or $\bar{\bullet}$'s if $c \leq 0$; see Example 4.17. Note that we may recover the full local rule diagram from its top row $\lambda \xrightarrow{d} \nu$ together with the \bullet or $\bar{\bullet}$ markings. Roughly speaking, when computing $\mathcal{P}(T)$, instead of directly computing $\text{BK}_1(T), \text{BK}_2 \circ \text{BK}_1(T), \dots$, we may track the positions of the \bullet 's or $\bar{\bullet}$'s in the top row. To formalize this, we introduce *jeu de taquin* for fluctuating tableaux. We again begin with a definition via local rules, and then give a tableau-theoretic description, generalizing the description in the generalized oscillating case from [Pat19].

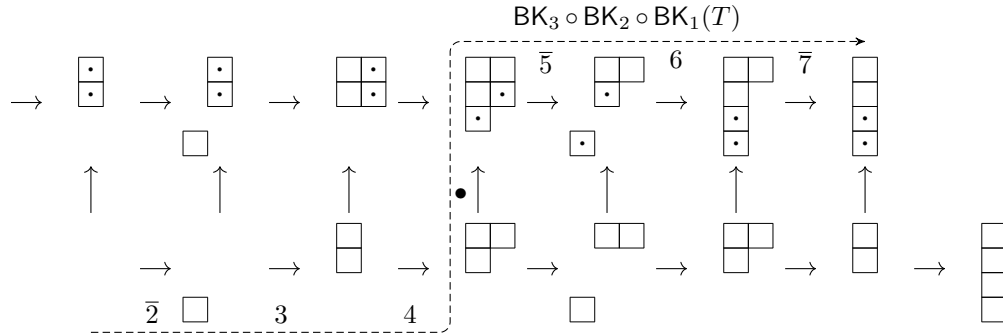
Example 4.17. In the following local rule associated to $1111\bar{2} \xrightarrow{4} 2221\bar{1} \xrightarrow{3} 3322\bar{1}$, we mark the 4 added cells in the vertical arrows with \bullet 's:



Definition 4.18. Given a fluctuating tableau $T = \lambda^0 \rightarrow \dots \rightarrow \lambda^n$, let $\text{jdt}_i(T)$ be the diagram of $\text{BK}_i \circ \dots \circ \text{BK}_1(T)$, where the first i steps are labeled $\pm 2, \dots, \pm(i+1)$'s, the $(i+1)$ st step is labeled with \bullet 's or $\bar{\bullet}$'s, and the remaining steps are labeled with $\pm(i+2), \dots, \pm n$'s.

From this definition, we see immediately that $\mathcal{P}(T)$ is obtained from $\text{jdt}_{n-1}(T)$ by replacing \bullet or $\bar{\bullet}$ with $n+1$ or $\bar{n}+1$, respectively, and then decreasing the absolute value of all entries by 1.

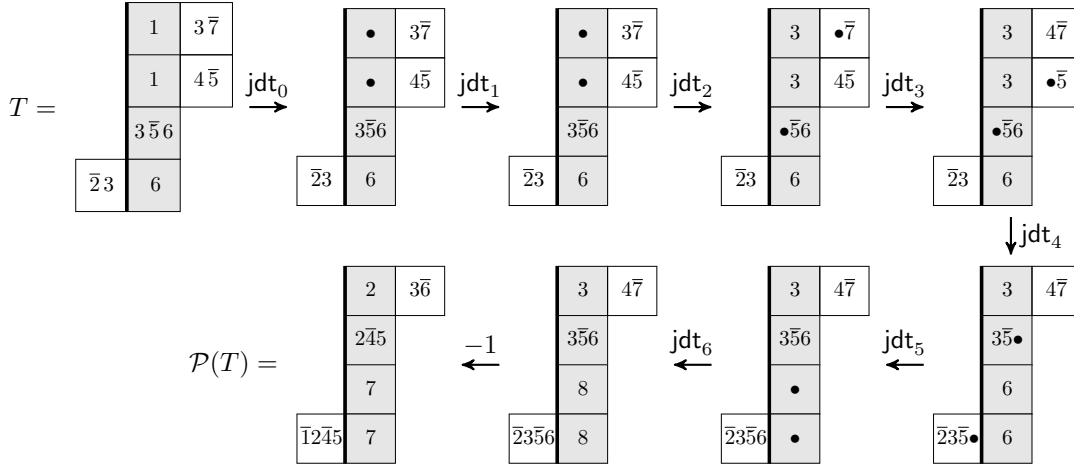
Example 4.19. In the first two rows of $\mathcal{PE}\text{-diagram}(T)$ for our fluctuating tableau T from Figure 2, we record the location of the two \bullet 's in the top row:



Here, we have marked the labels to be used when computing $\text{jdt}_3(T)$, which is

	3	$4\bar{7}$
	3	$\bullet\bar{5}$
	$\bullet\bar{5}6$	
$\bar{2}3$	6	

Putting these calculations together, we compute $\mathcal{P}(T)$ as follows:



We may encode the changes in the positions of the \bullet 's or $\bar{\bullet}$'s using the following combinatorial notion. Here, we imagine we have some fluctuating tableau T that has been labeled using the ordering $i-1 < \bullet < i$. We also import the notions of open cells from Definition 4.7.

Definition 4.20. The *jeu de taquin slides* for jdt_{i-1} on fluctuating tableaux labeled by $1 < 2 < \dots < i-1 < \bullet < i < \dots$ and their negatives are given by the following rules. See Figure 6 for schematic diagrams.

- (a) \bullet 's first move right to swap places with i 's, then move down as far as possible by swapping places with i 's.
- (b) $\bar{\bullet}$'s first move left to swap places with \bar{i} 's, then move up as far as possible by swapping places with \bar{i} 's.
- (c) $\bullet\bar{i}$ pairs move down as far as possible into open cells, and then they move left one column before becoming $\bar{i}\bullet$ pairs.
- (d) $\bar{\bullet}i$ pairs move up as far as possible into open cells, and then move right one column before becoming $i\bar{\bullet}$ pairs.

All other entries are left unchanged. This results in a fluctuating tableau whose diagram is labeled by $1 < 2 < \dots < i < \bullet < i+1 < \dots$ and their negatives.

The following is straightforward by comparing jeu de taquin slides, the tableau-theoretic description of Bender–Knuth involutions, and the properties of local rule diagrams.

Lemma 4.21. *Jeu de taquin slides result in fluctuating tableaux labeled by $1 < 2 < \dots < i < \bullet < i+1 < \dots$ and they encode local rules.*

Lemma 4.22. *Let T be a length n skew fluctuating tableau.*

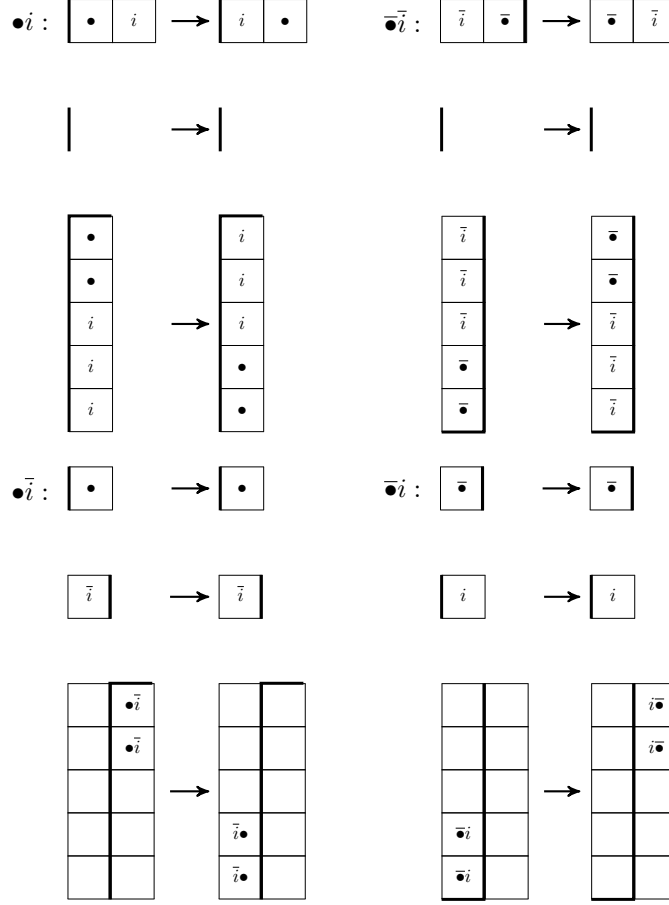


FIGURE 6. Jeu de taquin slides for jdt_{i-1} on fluctuating tableaux. In each case, the thick line indicates the boundary of the shape immediately before the \bullet . One may interpret the $\bullet i$ rules as first sliding \bullet 's right one cell past i 's, and then sliding \bullet 's down past i 's. The $\bullet \bar{i}$ rules instead “slide past” open cells and move left. The open cells in this case are simply those directly below $\bullet \bar{i}$'s, immediately right of the thick line, and without \bullet or \bar{i} .

- (i) $\mathcal{P}(T)$ is the result of replacing ± 1 's with $\pm \bullet$'s, using jeu de taquin slides $\text{jdt}_1, \dots, \text{jdt}_{n-1}$, replacing $\pm \bullet$'s with $\pm(n+1)$'s, and subtracting 1 from each entry's absolute value.
- (ii) $\mathcal{E}(T)$ is the result of first replacing ± 1 's with $\pm \bullet_n$'s, sliding them past $\pm n$'s, replacing ± 2 's with $\pm \bullet_{n-1}$'s, sliding them past $\pm n$'s, etc., and finally replacing $\pm \bullet_i$'s with $\pm i$'s.
- (iii) $\mathcal{E}^*(T)$ is the result of first replacing $\pm n$'s with $\pm \bullet_1$'s, sliding backwards past ± 1 's, replacing $\pm(n-1)$'s with $\pm \bullet_2$'s, sliding backwards past ± 1 's, etc., and finally replacing $\pm \bullet_i$'s with $\pm i$'s.

5. PROMOTION GRIDS AND PROMOTION MATRICES

Hopkins–Rubey [HR22, §4] attached certain decorations to promotion-evacuation diagrams of rectangular 3-row standard tableaux, which may be encoded as a permutation. We now extend this approach to arbitrary fluctuating tableaux with any number of rows.

5.1. Local rule grids. Given a local rule diagram, we may encode it as in Section 4.4 as an application of jeu de taquin involving \bullet 's or $\bar{\bullet}$'s and i 's or \bar{i} 's. We decorate the diagram as follows.

Definition 5.1. The *local rule grid* associated to an r -row fluctuating tableau local rule

$$(5.1) \quad \begin{array}{ccc} \lambda & \xrightarrow{d} & \nu \\ \uparrow c & & \uparrow c \\ \kappa & \xrightarrow{d} & \mu \end{array}$$

is a $|c| \times |d|$ grid M of intervals in $\{1, \dots, r-1\}$ defined as follows. First, encode the diagram as a jeu de taquin slide $S \rightarrow T$.

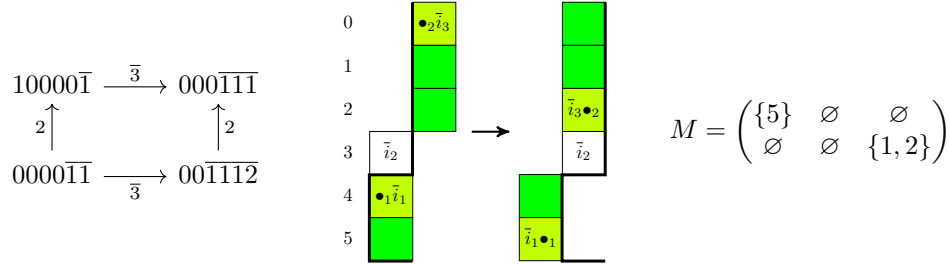
- ♦ If $c \geq 0$, number the \bullet 's in S and T from bottom to top as $\bullet_1, \dots, \bullet_c$.
- ♦ If $c \leq 0$, number the $\bar{\bullet}$'s in S and T from top to bottom as $\bar{\bullet}_1, \dots, \bar{\bullet}_{-c}$.
- ♦ If $d \geq 0$, number the i 's in S and T from top to bottom as i_1, \dots, i_d .
- ♦ If $d \leq 0$, number the \bar{i} 's in S and T from bottom to top as $\bar{i}_1, \dots, \bar{i}_{-d}$.

Index rows of S and T from 0 to $r-1$ from the top down. Consider cases based on the signs of c and d :

- ♦ $(0 \leq c, d)$: If \bullet_a swaps vertically with i_b , let $M_{ab} = \{j\}$ where j is the row of \bullet_a after the slide.
- ♦ $(c, d \leq 0)$: If $\bar{\bullet}_a$ swaps vertically with \bar{i}_b , let $M_{ab} = \{j\}$ where j is the row of $\bar{\bullet}_a$ before the slide.
- ♦ $(d \leq 0 \leq c)$: If $\bullet_a \bar{i}_b$ slides from row j in S to row k in T , let $M_{ab} = (j, k]$.
- ♦ $(c \leq 0 \leq d)$: If $\bar{\bullet}_a i_b$ slides from row k in S to row j in T , let $M_{ab} = (j, k]$.

We draw a local rule grid by writing the matrix M in the center of the local rule diagram.

Example 5.2. Consider the following local rule diagram, its corresponding jeu de taquin diagram, and the resulting local rule grid:



Here, the moving cells have been shaded in light green and the open cells have been shaded in darker green . The pair $\bullet_2 \bar{i}_3$ moved from row 0 to row 2, so $M_{23} = (0, 2] = \{1, 2\}$.

We will generally draw this local rule grid as

$$\begin{array}{ccc} 10000\bar{1} & \xrightarrow{\bar{3}} & 000\bar{1}\bar{1}\bar{1} \\ \uparrow 2 & \begin{smallmatrix} 5 & \cdot & \cdot \\ \cdot & \cdot & \cdot \end{smallmatrix} & \uparrow 2 \\ 0000\bar{1}\bar{1} & \xrightarrow{\bar{3}} & 00\bar{1}\bar{1}\bar{1}\bar{2} \end{array}$$

drawing M in the center of its local rule diagram, dropping brackets on singleton sets, and shrinking empty sets to dots.

Definition 5.3. The *triangular grids* U and L associated to the r -row fluctuating tableau diagrams

$$(5.2) \quad \begin{array}{ccc} \emptyset & \xrightarrow{c} & \nu \\ & \uparrow c & \\ \emptyset & & \end{array} \quad \text{and} \quad \begin{array}{ccc} \emptyset & & \\ \uparrow c & & \\ \kappa & \xrightarrow{c} & \emptyset \end{array}$$

respectively, are defined as follows. The triangular grid U is an upper triangular grid with c rows and c columns whose entries are elements of $\{0, \dots, r\}$. Conversely, L is a lower triangular grid that also has c rows and c columns and entries that are elements of $\{0, \dots, r\}$.

If $c = 4$, we have

$$U = \begin{array}{cccc} 0 & 1 & 2 & 3 \\ & 0 & 1 & 2 \\ & & 0 & 1 \\ & & & 0 \end{array} \quad \text{and} \quad L = \begin{array}{cccc} & & & r \\ & & r-1 & r \\ & r-2 & r-1 & r \\ & r-3 & r-2 & r-1 & r \end{array}$$

while in general, for $c \geq 0$, we have $U_{ij} = j - i$ whenever $1 \leq i \leq j \leq c$, and $L_{ij} = r - i + j$ whenever $1 \leq j \leq i \leq c$. If $c = -4$, we have

$$U = \begin{array}{cccc} r & r-1 & r-2 & r-3 \\ & r & r-1 & r-2 \\ & & r & r-1 \\ & & & r \end{array} \quad \text{and} \quad L = \begin{array}{cccc} & & & 0 \\ & & 1 & 0 \\ & 2 & 1 & 0 \\ & 3 & 2 & 1 & 0 \end{array}$$

while in general, for $c \leq 0$, we have $U_{ij} = r - j + i$ whenever $1 \leq i \leq j \leq -c$, and $L_{ij} = i - j$ whenever $1 \leq j \leq i \leq -c$.

Lemma 5.4. *Given $\kappa \xrightarrow{c} \lambda$ and M in (5.1), we can infer the rest of the local rule diagram. Similarly, the upper triangular grid U in (5.2) uniquely determines c and ν , while the lower triangular grid L in (5.2) uniquely determines c and κ .*

Proof. For the first claim, we know the location of \bullet_a 's or $\bar{\bullet}_a$'s in S . If \bullet_a or $\bar{\bullet}_a$ does not move, then $M_{ab} = \emptyset$ for all b . If \bullet_a or $\bar{\bullet}_a$ does move, we may infer where it moves by examining M_{ab} for all b . Hence we know the locations of the $\pm\bullet$'s in S and T , and thereby the locations of the $\pm i$'s in S and T . Thus we may infer ν , which lets us infer μ . The other claims are similar but easier. \square

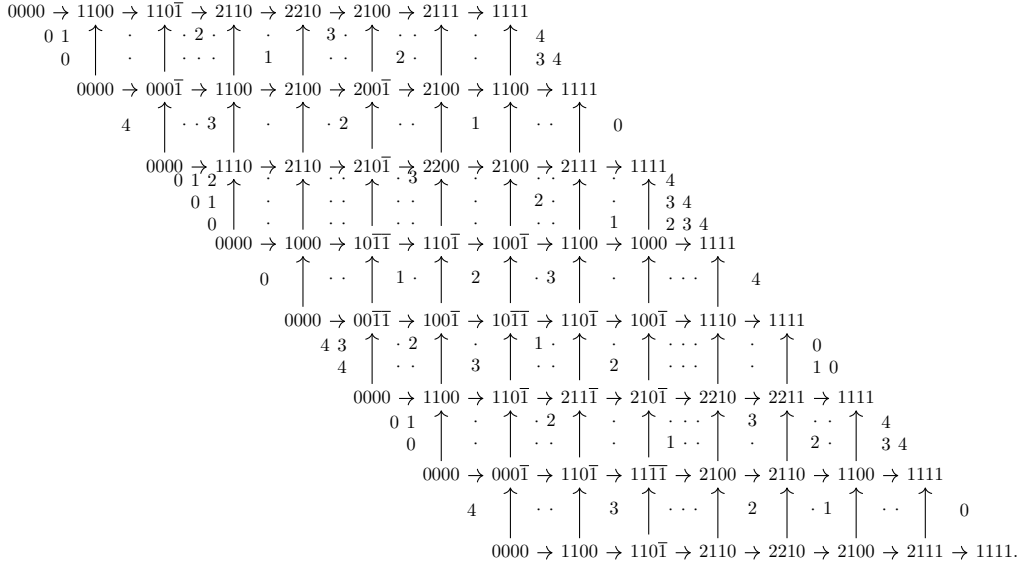
5.2. Promotion grids. We now glue together some local rule grids and triangular grids to form a single block grid.

Definition 5.5. Let \mathcal{D} be a growth diagram for an r -row non-skew fluctuating tableau T , for example \mathcal{P} -diagram(T), \mathcal{E} -diagram(T), \mathcal{E}^* -diagram(T), or \mathcal{PE} -diagram(T). The \mathcal{D} -grid of \mathcal{D} is the block grid $\mathbf{M}_{\mathcal{D}}$ whose blocks are the local rule grids of \mathcal{D} and appropriately-sized triangular grids.

This definition can be extended to handle skew fluctuating tableaux; however, the definitions of the triangular grids needed become significantly more complicated and we do not currently have an application of the extra generality such a definition would give, so we omit the details here.

Notation 5.6. We use the abbreviations $\mathbf{M}_{\mathcal{P}}(T) = \mathbf{M}_{\mathcal{P}\text{-diagram}(T)}$, $\mathbf{M}_{\mathcal{E}}(T) = \mathbf{M}_{\mathcal{E}\text{-diagram}(T)}$, $\mathbf{M}_{\mathcal{E}^*}(T) = \mathbf{M}_{\mathcal{E}^*\text{-diagram}(T)}$, and $\mathbf{M}_{\mathcal{PE}}(T) = \mathbf{M}_{\mathcal{PE}\text{-diagram}(T)}$. We will also use the names *promotion grid*, *evacuation grid*, etc., with the obvious meanings.

Example 5.7. For the fluctuating tableau T from Figure 2, we write the blocks of $\mathbf{M}_{\mathcal{PE}}(T)$ in \mathcal{PE} -diagram(T):



The lemma below follows directly from the definitions.

Lemma 5.8. *Consider reading a row of $\mathbf{M}_{\mathcal{PE}}(T)$ either from left to right if the label on the first arrow is positive or from right to left if the label on the first arrow is negative, skipping empty entries. The result is a sequence of intervals $[0, i_1], (i_1, i_2], \dots, (i_k, r]$ where $0 \leq i_1 < i_2 < \dots < i_k \leq r - 1$.*

Since in Example 5.7, all nonempty intervals are single elements, the above lemma says all nonempty entries in a row of the promotion-evacuation grid are sequentially 0, 1, 2, 3, 4 or 4, 3, 2, 1, 0, according to whether boxes are added or removed in the first step.

Evacuation grids may be used as alternate encodings of fluctuating tableaux as follows. We will shortly use a similar encoding in the rectangular case, with particularly desirable properties.

Theorem 5.9. *The map $T \mapsto (\mathbf{M}_{\mathcal{E}}(T), \text{type}(T))$ is injective.*

Proof. We may infer the block sizes of $\mathbf{M}_{\mathcal{E}}(T)$ from the type of T . We may fill \mathcal{E} -diagram(T) diagonal by diagonal by Lemma 5.4. Finally, we may read off T from the top row of \mathcal{E} -diagram(T). \square

Note that we may infer $\text{type}(T)$ from $\mathbf{M}_{\mathcal{E}}(T)$ if we track the blocks of $\mathbf{M}_{\mathcal{E}}(T)$. In this sense, we may entirely encode fluctuating tableaux of a fixed shape in terms of the block grid $\mathbf{M}_{\mathcal{E}}(T)$.

We now consider the effect on a \mathcal{D} -grid of oscillizing the growth diagram \mathcal{D} .

Lemma 5.10. *If \mathcal{D} is a skew fluctuating growth diagram, then*

$$\mathbf{M}_{\mathcal{D}} = \mathbf{M}_{\text{osc}(\mathcal{D})}.$$

Proof. One may check that the \mathcal{D} -grids in (5.1) have been defined so that the \mathcal{D} -grid agrees with the \mathcal{D} -grid of its oscillization. It is easy to see that the same is true for (5.2). \square

We now describe the effect of various diagram involutions on \mathcal{D} -grids. We will need these observations to determine the order of promotion on rectangular fluctuating tableaux.

Definition 5.11. Given any grid M , let M^\top be the *transpose* of M and let M^\perp be the *anti-diagonal transpose* of M .

Note that the composite of the transpose and anti-diagonal transpose is rotation by 180° . Recall that by convention τ and ε act on growth diagrams by applying τ and ε to each edge and rotating the result by 180° .

Lemma 5.12. *Suppose \mathcal{D} is an r -row fluctuating growth diagram. Then:*

- (i) $\mathbf{M}_{\mathcal{D}^\perp} = \mathbf{M}_{\mathcal{D}}^\perp$,
- (ii) $\mathbf{M}_{\tau(\mathcal{D})} = \mathbf{M}_{\mathcal{D}}^{\top\perp}$,
- (iii) $\mathbf{M}_{\varpi(\mathcal{D})} = r - \mathbf{M}_{\mathcal{D}}$,
- (iv) $\mathbf{M}_{\varepsilon(\mathcal{D})} = r - \mathbf{M}_{\mathcal{D}}^{\top\perp}$.

Here $(r - \mathbf{N})_{ab} := \{r - i : i \in \mathbf{N}_{ab}\}$.

Proof. For (i), the roles of \bullet , i and S, T are interchanged between the two diagrams. The result then follows by examining the symmetry in the definition of the promotion grid.

For (ii), after applying τ to the local rule, we rotate the diagram 180° . If we encode the original diagram in jeu de taquin with $S \rightarrow T$, the new diagram encoded via jeu de taquin as $S' \rightarrow T'$ where S' is the same as T and T' is the same as S after the replacements $\bar{\bullet}_a \leftrightarrow \bullet_{c+1-a}$ and $\bar{i}_b \leftrightarrow i_{d+1-b}$. The indices $\{j\}$ and $\{j, k\}$ are preserved. Hence $\tau(M)_{ab} = M_{c+1-a, d+1-b} = (M^{\top\perp})_{ab}$.

For (iii), applying ϖ to a local rule diagram has the effect of rotating each individual generalized partition 180° . Correspondingly, S'' is the same as S and T'' is the same as T but rotated 180° and with the replacements $\bullet_a \leftrightarrow \bar{\bullet}_a$, $i_b \leftrightarrow \bar{i}_b$. Moreover, row indices are reversed according to $j \leftrightarrow r - j$.

For (iv), we compose τ and ϖ . \square

The lemma below follows straightforwardly from Lemma 5.12.

Lemma 5.13. *On r -row skew fluctuating tableaux, we have the following.*

- (i) $\mathbf{M}_{\mathcal{E}}(\mathcal{E}(T)) = \mathbf{M}_{\mathcal{E}}(T)^\perp$, $\mathbf{M}_{\mathcal{E}^*}(\mathcal{E}^*(T)) = \mathbf{M}_{\mathcal{E}^*}(T)^\perp$
- (ii)

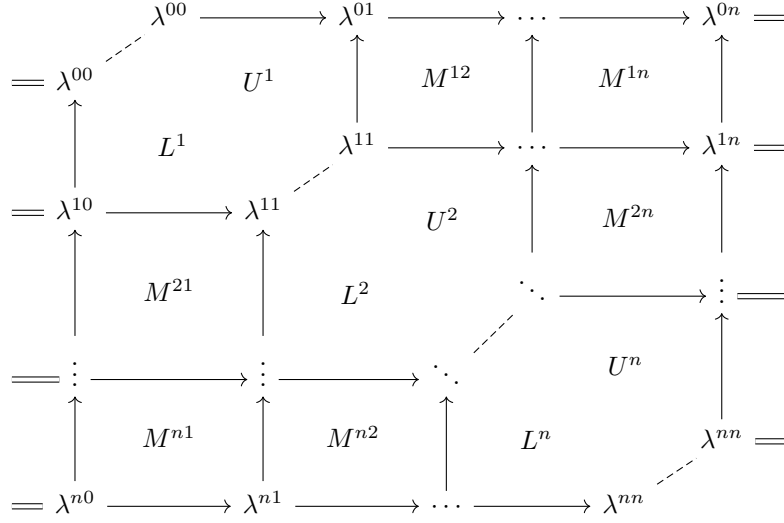
$$\begin{aligned} \mathbf{M}_{\mathcal{E}}(\tau(T)) &= \mathbf{M}_{\mathcal{E}^*}(T)^{\top\perp} & \mathbf{M}_{\mathcal{E}^*}(\tau(T)) &= \mathbf{M}_{\mathcal{E}}(T)^{\top\perp} \\ \mathbf{M}_{\mathcal{E}}(\varpi(T)) &= r - \mathbf{M}_{\mathcal{E}}(T) & \mathbf{M}_{\mathcal{E}^*}(\varpi(T)) &= r - \mathbf{M}_{\mathcal{E}^*}(T) \\ \mathbf{M}_{\mathcal{E}}(\varepsilon(T)) &= r - \mathbf{M}_{\mathcal{E}^*}(T)^{\top\perp} & \mathbf{M}_{\mathcal{E}^*}(\varepsilon(T)) &= r - \mathbf{M}_{\mathcal{E}}(T)^{\top\perp} \end{aligned}$$

- (iii) $\mathbf{M}_{\mathcal{PE}}(\varpi(T)) = r - \mathbf{M}_{\mathcal{PE}}(T)$

5.3. Promotion matrices. Next we encode $\mathbf{M}_{\mathcal{PE}}(T)$ in a square block matrix.

Definition 5.14. The *promotion matrix* of an r -row fluctuating tableau T of length n is the $n \times n$ block matrix $\mathbf{M}(T)$ whose upper triangle is $\mathbf{M}_{\mathcal{E}}(T)$ and whose lower triangle is $\mathbf{M}_{\mathcal{E}^*}(\mathcal{E}^*(T))$. Entries on the main diagonal are the union of the entries from the main diagonals of the two triangles, reduced modulo r (and hence are always 0).

We visualize $\mathbf{M}(T)$ by “wrapping around” \mathcal{PE} -diagram(T) to form a square matrix:



Here, U^i is upper triangular and L^i is lower triangular, as in Definition 5.3, and they are combined in $\mathbf{M}(T)$. We will refer to the square grid constructed from U^i and L^i as M^{ii} for consistency with the indexing of the other blocks of $\mathbf{M}(T)$. Note that the entries in $\mathbf{M}_{\mathcal{PE}}(T)$ cyclically increment or decrement when reading across any given row in the sense of Lemma 5.8.

Example 5.15. For the fluctuating tableau T in Figure 2, $\text{type}(T) = (2, -1, 3, 1, -2, 2, -1)$ and the promotion matrix is

$$\mathbf{M}(T) = \begin{pmatrix} 0 & 1 & \cdot & \cdot & 2 & \cdot & \cdot & 3 & \cdot & \cdot & \cdot & \cdot \\ 3 & 0 & \cdot & \cdot & \cdot & \cdot & 1 & \cdot & \cdot & 2 & \cdot & \cdot \\ \cdot & \cdot & 0 & \cdot & \cdot & 3 & \cdot & \cdot & 2 & \cdot & \cdot & 1 \\ \cdot & \cdot & \cdot & 0 & 1 & 2 & \cdot & \cdot & \cdot & \cdot & 3 & \cdot \\ 2 & \cdot & \cdot & 3 & 0 & 1 & \cdot & \cdot & \cdot & \cdot & \cdot & \cdot \\ \cdot & \cdot & 1 & 2 & 3 & 0 & \cdot & \cdot & \cdot & \cdot & \cdot & \cdot \\ \cdot & 3 & \cdot & \cdot & \cdot & \cdot & 0 & \cdot & \cdot & 1 & \cdot & 2 \\ 1 & \cdot & \cdot & \cdot & \cdot & \cdot & \cdot & 0 & 3 & \cdot & 2 & \cdot \\ \cdot & \cdot & 2 & \cdot & \cdot & \cdot & \cdot & 1 & 0 & \cdot & \cdot & 3 \\ \cdot & 2 & \cdot & \cdot & \cdot & \cdot & 3 & \cdot & \cdot & 0 & 1 & \cdot \\ \cdot & \cdot & \cdot & 1 & \cdot & \cdot & \cdot & 2 & \cdot & 3 & 0 & \cdot \\ \cdot & \cdot & 3 & \cdot & \cdot & \cdot & 2 & \cdot & 1 & \cdot & \cdot & 0 \end{pmatrix}.$$

By Lemma 5.13(iii), we have

$$(5.3) \quad \mathbf{M}(\varpi(T)) = r - \mathbf{M}(T).$$

The effects of the other fundamental involutions in general are more complex. They can however be easily described in the case that evacuation and dual evacuation coincide.

Lemma 5.16. *The following are equivalent on r -row fluctuating tableaux:*

- (i) $\mathcal{E}(T) = \mathcal{E}^*(T)$
- (ii) $\mathbf{M}(\mathcal{E}(T)) = \mathbf{M}(T)^\perp$
- (iii) $\mathbf{M}(\mathcal{E}^*(T)) = \mathbf{M}(T)^\perp$
- (iv) $\mathbf{M}(\tau(T)) = \mathbf{M}(T)^{\top\perp}$
- (v) $\mathbf{M}(\varepsilon(T)) = r - \mathbf{M}(T)^{\top\perp}$

Proof. By (3.5) and Theorem 5.9, we have (i) if and only if

$$(5.4) \quad \mathbf{M}_{\mathcal{PE}}(T) = \mathbf{M}_{\mathcal{E}}(T) \parallel \mathbf{M}_{\mathcal{E}^*}(T),$$

where \parallel denotes concatenating the grids and identifying the column where equality holds. By Lemma 3.13, we may replace T in (5.4) with $\tau(T)$ or $\varepsilon(T)$ while remaining equivalent to (i). Using Lemma 5.13, we obtain

$$\begin{aligned} \mathbf{M}_{\mathcal{E}}(\tau(T)) \parallel \mathbf{M}_{\mathcal{E}^*}(\tau(T)) &= \mathbf{M}_{\mathcal{E}^*}(T)^{\top\perp} \parallel \mathbf{M}_{\mathcal{E}}(T)^{\top\perp} \\ &= (\mathbf{M}_{\mathcal{E}}(T) \parallel \mathbf{M}_{\mathcal{E}^*}(T))^{\top\perp} \\ &= \mathbf{M}(T)^{\top\perp}. \end{aligned}$$

In this way, (i), (iv), and (v) are equivalent. The argument for (ii) and (iii) is essentially identical. \square

Lemma 5.17. *The following are equivalent on r -row skew fluctuating tableaux:*

- (i) $\mathcal{E}(T) = \varepsilon(T)$
- (ii) $\mathcal{E}^*(T) = \varepsilon(T)$
- (iii) $\mathbf{M}(T) = r - \mathbf{M}(T)^{\top}$

Proof. We have seen the equivalence of (i) and (ii) in Lemma 3.14. For the rest, by (3.5) we have (iii) if and only if

$$\mathbf{M}_{\mathcal{E}^*}(\mathcal{E}^* \circ \mathcal{E}(T)) = r - \mathbf{M}_{\mathcal{E}}(T)^{\top}.$$

Take the anti-diagonal transpose of both sides. Now

$$\mathbf{M}_{\mathcal{E}^*}(\mathcal{E}^* \circ \mathcal{E}(T))^{\perp} = \mathbf{M}_{\mathcal{E}^*}(\mathcal{E}(T))$$

by Lemma 5.13, and likewise

$$(r - \mathbf{M}_{\mathcal{E}}(T)^{\top})^{\perp} = r - \mathbf{M}_{\mathcal{E}}(T)^{\top\perp} = \mathbf{M}_{\mathcal{E}^*}(\varepsilon(T)).$$

Note that, by Theorem 5.9, $\mathbf{M}_{\mathcal{E}^*}(\mathcal{E}(T)) = \mathbf{M}_{\mathcal{E}^*}(\varepsilon(T))$ is equivalent to (i), completing the proof. \square

5.4. Reduced promotion matrices. We now describe an alternate encoding of the promotion matrices $\mathbf{M}(T)$. This encoding directly corresponds to a crystal-theoretic interpretation given in Section 8.5.

Definition 5.18. The *reduced promotion matrices* of an r -row fluctuating tableau T of length n are the $n \times n$ matrices $\overline{\mathbf{M}}^i(T)$ (for $0 \leq i \leq r-1$) with entries in $\mathbb{Z}_{\geq 0}$ defined by

$$\overline{\mathbf{M}}^i(T)_{uv} = \#\{\text{entries in the block } M^{uv} \text{ of } \mathbf{M}(T) \text{ containing } i\}.$$

We have the following direct characterization of $\overline{\mathbf{M}}(T)_{uv}^i$ off the main diagonal.

Proposition 5.19. *Suppose we have a local rule diagram*

$$\begin{array}{ccc} \lambda & \longrightarrow & \nu \\ \uparrow & \overline{\mathbf{M}}^i & \uparrow \\ \kappa & \longrightarrow & \mu \end{array}$$

where $\lambda = \kappa + \mathbf{e}_A$, $\nu = \mu + \mathbf{e}_B$, and $\overline{\mathbf{M}}^i$ are the reduced promotion matrix entries. Then the $\overline{\mathbf{M}}^i$ are uniquely characterized by

$$(5.5) \quad \mathbf{e}_B = \mathbf{e}_A + \sum_{i=1}^{r-1} \overline{\mathbf{M}}^i(\mathbf{e}_{i+1} - \mathbf{e}_i).$$

Proof. Consider the jeu de taquin slides associated with this local rule diagram. Recall that the rows of fluctuating tableaux are indexed top-down from 0 to $r - 1$. Note that all elements of A and B have the same sign. If A, B consist of positive numbers, the \bullet 's begin in the rows indexed by $\{a - 1 : a \in A\}$ and end in the rows indexed by $\{b - 1 : b \in B\}$. If A, B consist of negative numbers, the $\bar{\bullet}$'s begin in the rows indexed by $\{-a - 1 : a \in A\}$ and end in the rows indexed by $\{-b - 1 : b \in B\}$. In the former case, $\bar{\mathbf{M}}^i$ counts the number of times a \bullet slides from row $i - 1$ to row i , which effectively removes \mathbf{e}_i from \mathbf{e}_A and adds \mathbf{e}_{i+1} to \mathbf{e}_B . In the latter case, $\bar{\mathbf{M}}^i$ counts the number of times a $\bar{\bullet}$ slides from row i to row $i - 1$, which effectively removes $\mathbf{e}_{i+1} = -\mathbf{e}_{i+1}$ from \mathbf{e}_A and adds $\mathbf{e}_i = -\mathbf{e}_i$ to \mathbf{e}_B . The net effect is the same in either case, and (5.5) follows by summing. Uniqueness follows from the fact that the $\mathbf{e}_{i+1} - \mathbf{e}_i$ are linearly independent. \square

The reduced promotion matrix analogue of Theorem 5.9 holds.

Theorem 5.20. *The map $T \mapsto (\bar{\mathbf{M}}^1(T), \dots, \bar{\mathbf{M}}^{r-1}(T), \text{type}(T))$ is injective.*

Proof. It suffices to show that Lemma 5.4 remains true given only the number of entries of each type in the promotion grids rather than the full promotion grids. We know the positions of the $\pm\bullet$'s and $\pm i$'s in S as well as the number of times some $\pm\bullet$ slides past each particular row. We may hence infer the final row of the bottommost \bullet or topmost $\bar{\bullet}$, and iteratively we may infer all final locations of $\pm\bullet$'s. The arguments for the other diagrams are similar. \square

Example 5.21. For the fluctuating tableau T from Figure 2, we have

$$\begin{aligned} \bar{\mathbf{M}}^0(T) &= \begin{pmatrix} 2 & 0 & 0 & 0 & 0 & 0 & 0 \\ 0 & 1 & 0 & 0 & 0 & 0 & 0 \\ 0 & 0 & 3 & 0 & 0 & 0 & 0 \\ 0 & 0 & 0 & 1 & 0 & 0 & 0 \\ 0 & 0 & 0 & 0 & 2 & 0 & 0 \\ 0 & 0 & 0 & 0 & 0 & 2 & 0 \\ 0 & 0 & 0 & 0 & 0 & 0 & 1 \end{pmatrix} & \bar{\mathbf{M}}^1(T) &= \begin{pmatrix} 1 & 0 & 0 & 1 & 0 & 0 & 0 \\ 0 & 0 & 0 & 0 & 0 & 0 & 1 \\ 0 & 1 & 2 & 0 & 0 & 0 & 0 \\ 0 & 0 & 0 & 0 & 0 & 1 & 0 \\ 1 & 0 & 0 & 0 & 1 & 0 & 0 \\ 0 & 0 & 1 & 0 & 0 & 1 & 0 \\ 0 & 0 & 0 & 0 & 1 & 0 & 0 \end{pmatrix} \\ \bar{\mathbf{M}}^2(T) &= \begin{pmatrix} 0 & 0 & 1 & 0 & 0 & 1 & 0 \\ 0 & 0 & 0 & 0 & 1 & 0 & 0 \\ 1 & 0 & 2 & 0 & 0 & 0 & 0 \\ 0 & 0 & 0 & 0 & 0 & 0 & 1 \\ 0 & 1 & 0 & 0 & 0 & 1 & 0 \\ 1 & 0 & 0 & 0 & 1 & 0 & 0 \\ 0 & 0 & 0 & 1 & 0 & 0 & 0 \end{pmatrix} & \bar{\mathbf{M}}^3(T) &= \begin{pmatrix} 1 & 0 & 0 & 0 & 1 & 0 & 0 \\ 0 & 0 & 1 & 0 & 0 & 0 & 0 \\ 0 & 0 & 2 & 0 & 0 & 1 & 0 \\ 1 & 0 & 0 & 0 & 0 & 0 & 0 \\ 0 & 0 & 0 & 0 & 1 & 0 & 1 \\ 0 & 0 & 0 & 1 & 0 & 1 & 0 \\ 0 & 1 & 0 & 0 & 0 & 0 & 0 \end{pmatrix} \end{aligned}$$

These matrices should be compared to the matrix $\mathbf{M}(T)$ from Example 5.15.

6. PROMOTION PERMUTATIONS

We begin by transforming promotion matrices into promotion functions. We then show they have particularly nice properties in the rectangular case and prove our main result, Theorem 6.7.

Definition 6.1. The *promotion functions* of an r -row fluctuating tableau T are defined as follows. Let t be the sum of the absolute values of the components of $\text{type}(T)$, so that $\mathbf{M}(T)$ is $t \times t$. For all $0 \leq i \leq r - 1$, each row of $\mathbf{M}(T)$ has a unique entry containing i . Set

$$\begin{aligned} \text{prom}_i(T) &: [t] \rightarrow [t] \\ \text{prom}_i(T)(a) &= b \quad \text{whenever } i \in \mathbf{M}(T)_{ab}. \end{aligned}$$

For symmetry, we define $\text{prom}_r(T) := \text{prom}_0(T)$.

Example 6.2. For the fluctuating tableau T from Figure 2 with promotion matrix found in Example 5.15, all the promotion functions are permutations. Specifically, we have

$$\begin{aligned}\text{prom}_0(T) &= \text{prom}_4(T) = \text{id} \\ \text{prom}_1(T) &= (1\ 2\ 7\ 10\ 11\ 4\ 5\ 6\ 3\ 12\ 9\ 8) \\ \text{prom}_2(T) &= (1\ 5)(2\ 10)(3\ 9)(4\ 6)(7\ 12)(8\ 11) \\ \text{prom}_3(T) &= (1\ 8\ 9\ 12\ 3\ 6\ 5\ 4\ 11\ 10\ 7\ 2).\end{aligned}$$

Remark 6.3. Note that $\text{prom}_0(T) = \text{id} = \text{prom}_r(T)$ are always trivial; they are included for overall consistency. Since the diagonal of $\mathbf{M}(T)$ is all zeros, all other $\text{prom}_i(T)$ are fixed-point free. Note that $\mathbf{M}(T)$ can be recovered from the collection $(\text{prom}_i(T))_{i=1}^{r-1}$ of all promotion functions. We will shortly see that, in the rectangular case, each $\text{prom}_i(T)$ is a permutation. In the rectangular case, we will therefore refer to promotion functions as *promotion permutations*.

We have the following relation between the promotion functions of T and the promotion functions of $\mathcal{P}(T)$.

Lemma 6.4. *We have*

$$\text{prom}_i(T)(u + |c_1|) = v + |c_1| \iff \text{prom}_i(\mathcal{P}(T))(u) = v$$

for all $1 \leq u, v \leq t - |c_1|$ and all $0 \leq i \leq r$.

Proof. By construction, the promotion-evacuation diagram of $\mathcal{P}(T)$ is obtained from that of T by cutting off the top row. Hence, the promotion matrix is obtained by cutting away the top c_1 rows and leftmost c_1 columns. The lemma follows. \square

It is well-known that the n th power of promotion on rectangular standard tableaux with n cells is the identity. Moreover, the effect of evacuation on such rectangular standard tableaux is the *reverse-complement* (see, e.g., [Hai92] for both of these facts), which in our terminology using lattice words is phrased as $L(\mathcal{E}(T)) = \varepsilon(L(T))$. These properties extend to rectangular fluctuating tableaux; for an example, see Figure 7.

Theorem 6.5. *Let T be a rectangular fluctuating tableau of length n . Then*

- (a) $\mathcal{P}^n(T) = T$
- (b) $L(\mathcal{E}(T)) = \varepsilon(L(T))$

Proof. In terms of tableaux, (b) is equivalent to $\mathcal{E}(T) = \varepsilon(T)$. By Lemma 3.14, (b) implies (a).

As for (b), we may use the switch_i involutions and Lemma 4.6 to reduce to the case when T is (transpose) semi-standard. In this case, (b) is a well-known consequence of the RSK algorithm; see, e.g., [PP21, Lemma 3.1] for details. An alternate crystal-theoretic proof is given in Section 8.6. \square

We obtain the following as a corollary.

Corollary 6.6. *All of the equivalent conditions in Lemma 5.16 and Lemma 5.17 hold for rectangular fluctuating tableaux.*

The following is the main result of the present work. Let $\sigma = (1\ 2 \cdots t)$ be the long cycle, and let $w_0 = (1, t)(2, t-1) \cdots$ be the longest element in the symmetric group \mathfrak{S}_t .

Theorem 6.7. *Let T be an r -row rectangular fluctuating tableau of type (c_1, \dots, c_n) where $|c_1| + \cdots + |c_n| = t$. Then for all $0 \leq i \leq r$:*

- (i) $\text{prom}_i(T)$ is a permutation
- (ii) $\text{prom}_i(T) = \text{prom}_{r-i}(T)^{-1}$
- (iii) $\text{prom}_i(\mathcal{P}(T)) = \sigma^{-|c_1|} \text{prom}_i(T) \sigma^{|c_1|}$
- (iv) $\text{prom}_i(\mathcal{E}(T)) = w_0 \text{prom}_i(T) w_0$

Proof. By Corollary 6.6, we have all the equivalent conditions of Lemma 5.16 and Lemma 5.17. Lemma 5.17(iii) implies (i) and (ii). Lemma 6.4 implies (iii). Finally, (iv) follows from Lemma 5.16(v) and the fact that, for any matrix M , we have $M^{\top\perp} = w_0 M w_0$, where w_0 is viewed as a permutation matrix. \square

Corollary 6.8. *If T is a rectangular fluctuating tableau with r rows and $1 \leq i \leq r-1$, then $\text{prom}_i(T)$ is a fixed-point free permutation. Moreover if r is even, then $\text{prom}_{r/2}(T)$ is a fixed-point free involution.*

Proof. This is an immediate consequence of (i) and (ii) in the above theorem and Remark 6.3. \square

We now describe how to obtain promotion permutations directly from a tableau without reference to promotion matrices.

Proposition 6.9. *Let $T \in \text{FT}(r, n)$ be a fluctuating tableau and $1 \leq i \leq r-1$. Then $\text{prom}_i(T)(b) \equiv |a| + b - 1 \pmod{n}$ if and only if a is the unique value that crosses the boundary between rows i and $i+1$ in the application of jeu de taquin promotion to $\mathcal{P}^{b-1}(\text{osc}(T))$.*

Proof. First, suppose T is of oscillating type. Consider repeatedly performing promotion on T via jeu de taquin with the convention that we do not relabel entries after promotion. Then $\mathbf{M}_{\mathcal{PE}}(T)$ records an i in row a , column b , when letter a or \bar{a} crosses the boundary between rows i and $i+1$ during the b th application of promotion to T . Since promotion actually decreases the absolute value of all entries by 1, the result follows in this case.

If T is not of oscillating type, we may instead consider $\text{osc}(T)$. By Lemma 5.10, $\mathbf{M}_{\mathcal{PE}}(T) = \mathbf{M}_{\mathcal{PE}}(\text{osc}(T))$, so the theorem follows from the previous case. \square

We end this section by describing properties of promotion permutations that determine the entries of the corresponding tableau. We will use the following lemma.

Lemma 6.10. *Given a fluctuating tableau T of r rows and $0 \leq i \leq r$, $\text{prom}_i(T) = \text{prom}_i(\text{osc}(T))$.*

Proof. Lemma 5.10 directly implies that $\mathbf{M}(T) = \mathbf{M}(\text{osc}(T))$, so the conclusion follows. \square

Definition 6.11. Let $\pi \in \mathfrak{S}_n$ be a permutation. A number $i \in [n]$ is an *antiexcedance* of π if $\pi^{-1}(i) > i$. We write $\text{Aexc}(\pi)$ for the set of antiexcedances of π . We say $i \in [n]$ is an *excedance* of π if it is neither an antiexcedance nor a fixed point.

Theorem 6.12. *Let $T \in \text{FT}(r)$ be a rectangular fluctuating tableau. Suppose $1 \leq i \leq r-1$.*

Then a is an antiexcedance of $\text{prom}_i(T)$ if and only if either a appears in the top i rows of $\text{osc}(T)$ or \bar{a} appears in the bottom $r-i$ rows of $\text{osc}(T)$. In particular, if T is a standard tableau, then the antiexcedances of $\text{prom}_i(T)$ are exactly the numbers in the first i rows of T .

Proof. By Lemma 6.10, we may assume $T = \text{osc}(T)$. We start by characterizing the excedances of $\text{prom}_i(T)$ instead of the antiexcedances. Since $\text{prom}_i(T)$ is fixed-point free by Corollary 6.8, the antiexcedances are the complementary set to the excedances.

If we write a permutation $\pi \in \mathfrak{S}_n$ as a permutation matrix by placing 1 in each position $(a, \pi(a))$, then the excedances of π are exactly the values $\pi(a)$ such that $(a, \pi(a))$ appears strictly above the main diagonal.

The upper triangle of $\mathbf{M}(T)$ is $\mathbf{M}_{\mathcal{E}}(T)$. Consider repeatedly performing promotion on T via jeu de taquin with the convention that we do not relabel entries after promotion and we do not replace \bullet or $\bar{\bullet}$ by a new number at the end of promotion. Then $\mathbf{M}_{\mathcal{E}}(T)$ records an i in row a , column b , when letter a or \bar{a} crosses the boundary between rows i and $i+1$ during the b th application of promotion to T . Note that during jeu de taquin, unbarred entries only move weakly up, while barred entries only move weakly down. But the entry a must eventually exit out the top if it exists. Otherwise, \bar{a} exists and must exit out the bottom. Hence, $\mathbf{M}_{\mathcal{E}}(T)$ will have an i in row a if and only if a appears strictly below row i in T or if \bar{a} appears weakly above row i in T . Thus, a is an excedance of $\text{prom}_i(T)$ if

and only if a fails the hypotheses of the theorem. Thus, a is an antiexcedance of $\text{prom}_i(T)$ if and only if either a appears in the top i rows of T or \bar{a} appears in the bottom $r - i$ rows of T . \square

Corollary 6.13. *Suppose $T \in \text{FT}(r, \mathcal{C})$. Then T is uniquely determined by its type together with the promotion permutations $(\text{prom}_i(T))_{i=1}^{\lfloor r/2 \rfloor}$.*

Proof. This follows by combining Theorem 6.7 with Theorem 6.12 after oscillizing the tableau. \square

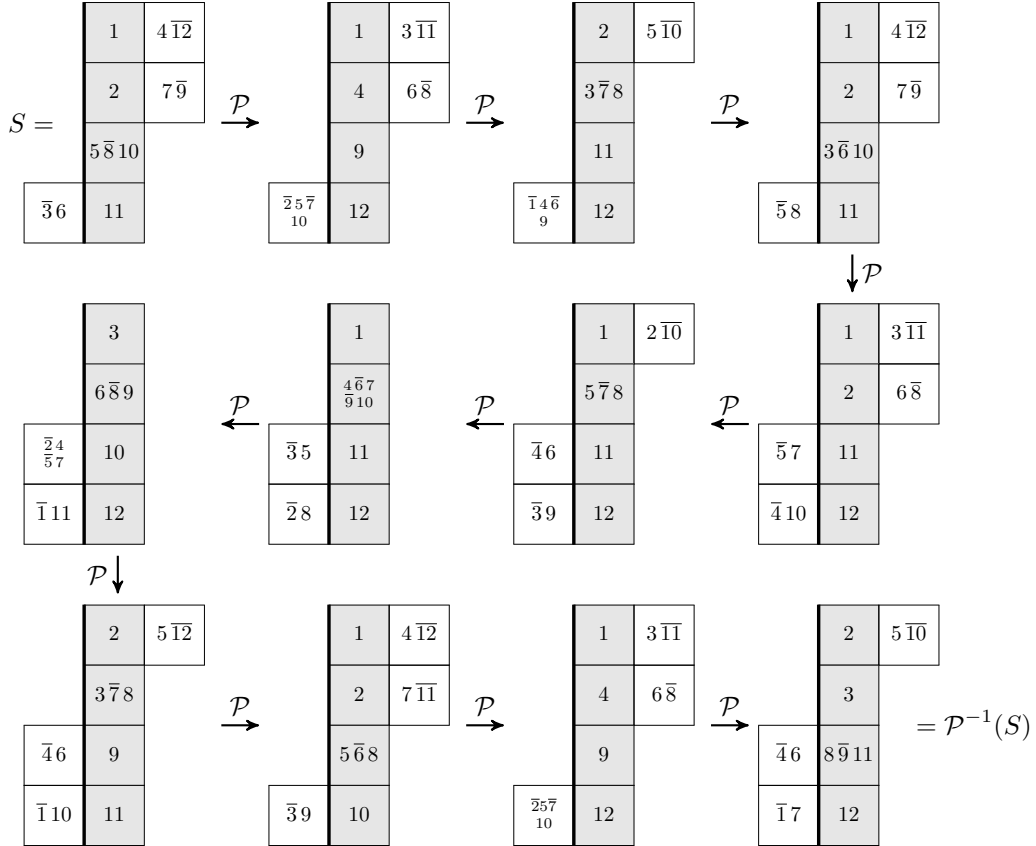


FIGURE 7. The full promotion orbit of $S := \text{osc}(T)$, where T is the fluctuating tableau from Figure 2.

Example 6.14. For T the fluctuating tableau from Figure 2, Figure 7 gives the full promotion orbit of $S := \text{osc}(T)$, which we use to illustrate Proposition 6.9 and Theorem 6.12. Proposition 6.9 allows us to write the promotion permutations of S by tracking entries that move between rows in applications of promotion. For example, $\text{prom}_1(T)(1) = 2$ because in the first promotion of Figure 7 the label 2 moves from row 2 to row 1 (and then becomes a 1). Similarly, $\text{prom}_1(T)(2) = 7$ because in the second promotion, the label 6 moves from row 2 to row 1 (and then becomes 5). More interestingly, $\text{prom}_1(T)(3) = 12$ because in the third promotion, the label $\overline{10}$ moves from row 1 to row 2 (and then becomes $\overline{9}$). Finally, we observe that $\text{prom}_2(T)(1) = 5$ because in the first promotion, the label 5 moves from row 3 to row 2 (and then becomes 4). The reader may enjoy recomputing the rest of Example 6.2 by analyzing Figure 7 and applying Proposition 6.9.

The antiexcedances of $\text{prom}_1(T)$ are 1, 3, 4, 8, 9. Note that 1 and 4 are the positive entries in row 1 of S , while $\overline{3}$, $\overline{8}$, and $\overline{9}$ are the negative entries in rows 2, 3, and 4 of S . The antiexcedances of

of $\text{prom}_2(T)$ are 1, 2, 3, 4, 7, 8. Note that 1, 2, 4 and 7 are the positive entries in rows 1 and 2, while $\bar{3}$ and $\bar{8}$ are the negative entries in rows 3, and 4. Finally, the antiexcedances of $\text{prom}_3(T)$ are 1, 2, 3, 4, 5, 7, 10. Note that 1, 2, 4, 5, 7, 10 are the positive entries in rows 1, 2, and 3, while $\bar{3}$ is the negative entry in row 4.

Remark 6.15. For $r > 2$, we do not know an intrinsic characterization of the tuples $(\text{prom}_i(T))_{i=0}^r$ that can arise for T an r -row rectangular fluctuating tableau. Necessary conditions include the fixed point conditions in Corollary 6.8, the row increasing conditions from Lemma 5.8, the symmetry Theorem 6.7(ii), and the nesting of the antiexcedance sets

$$\begin{aligned} \{a \in \text{Aexc}(\text{prom}_i(T)) : a > 0\} &\subseteq \{a \in \text{Aexc}(\text{prom}_{i+1}(T)) : a > 0\} \\ \{a \in \text{Aexc}(\text{prom}_{i+1}(T)) : a < 0\} &\subseteq \{a \in \text{Aexc}(\text{prom}_i(T)) : a < 0\} \end{aligned}$$

from Theorem 6.12. See Remark 7.3 for further related discussion.

7. DIHEDRAL MODELS OF PROMOTION AND EVACUATION

Recall that \mathcal{P} and \mathcal{E} generate an infinite dihedral action on skew fluctuating tableaux (see Lemma 3.12). By Theorem 6.5, $\mathcal{P}^n = \text{id}$ on rectangular fluctuating tableaux of length n , so there is a non-obvious action of the dihedral group of order $2n$ on such tableaux by promotion and evacuation. In this section, we use the preceding constructions to give a pictorial model of this dihedral action where \mathcal{P} corresponds to rotation and \mathcal{E} corresponds to reflection.

Let

$$\langle \text{rot}, \text{refl} \mid \text{rot}^n = \text{refl}^2 = 1, \text{rot} \circ \text{refl} = \text{refl} \circ \text{rot}^{-1} \rangle$$

be the dihedral group of symmetries of the regular n -gon, where rot acts as rotation by $2\pi/n$ and refl acts as reflection through a fixed axis which passes through the midpoint of an edge. For a given type $\underline{c} = (c_1, \dots, c_n)$ with $|c_1| + \dots + |c_n| = t$, this group acts on the set of tuples of maps

$$(f_i : [t] \rightarrow [t])_{i=0}^r$$

by

$$\begin{aligned} \text{rot}^k \cdot (f_i) &:= (\sigma^{-|c_1| - \dots - |c_k|} \circ f_i \circ \sigma^{|c_1| + \dots + |c_k|}) \quad \text{if } 1 \leq k \leq n \\ \text{refl} \cdot (f_i) &:= (w_0 \circ f_i \circ w_0)_{i=0}^{r-1}. \end{aligned}$$

Combining Theorem 5.9 and Theorem 6.7 gives the following.

Corollary 7.1. *The inclusion*

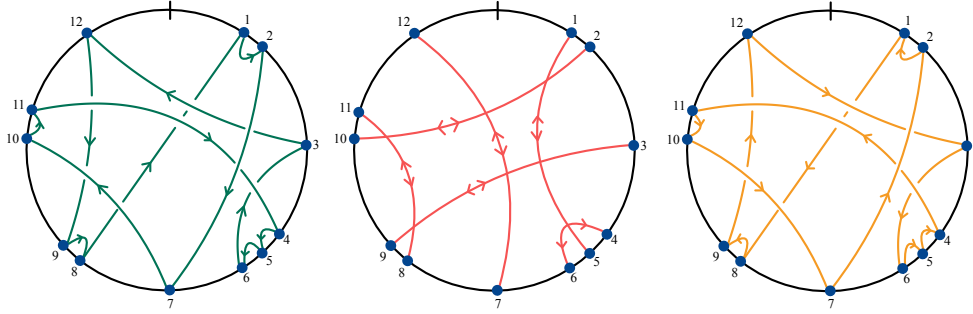
$$\Phi(T) := (\text{prom}_i(T))_{i=0}^r$$

from r -row rectangular fluctuating tableaux of length n and type \underline{c} to tuples of permutations intertwines promotion and evacuation with the action of the dihedral group of order $2n$:

$$\begin{aligned} \Phi(\mathcal{P}(T)) &= \text{rot} \cdot \Phi(T) \\ \Phi(\mathcal{E}(T)) &= \text{refl} \cdot \Phi(T). \end{aligned}$$

We may encode $\Phi(T)$ in terms of a diagram on a disk as in the following example. Place t vertices on the circumference in n equally-spaced groups of size $|c_1|, \dots, |c_n|$ in clockwise order. Place a directed edge from a to b with color i if $\text{prom}_i(T)(a) = b$. Promotion corresponds to counterclockwise rotation by $2\pi/n$ and evacuation corresponds to reflection across the diameter passing midway between the 1st and n th groups.

Example 7.2. For the fluctuating tableau T from Figure 2, the diagrams of the promotion permutations of T are as follows:



Here we have drawn the prom_i diagrams separately for clarity and included only $i = 1, 2, 3$ from left to right, though they rotate and reflect simultaneously. The action of \mathcal{P} corresponds to counterclockwise rotation by an angle of $2\pi/7$, while that of \mathcal{E} corresponds to reflection across the vertical axis. The fundamental involution ϖ corresponds to reversing the direction of the arrows, ε agrees with \mathcal{E} , and the time reversal involution τ corresponds to both reflecting the diagrams and reversing the direction of the arrows.

To reduce the number of vertices and edges, one could choose to combine the vertices in each group into a single vertex, and then additionally delete any loops formed by this process. This simplification is related to the reduced promotion matrices of Section 5.4.

Remark 7.3. This graphical model allows one to directly “see” the dihedral action of promotion and evacuation on rectangular fluctuating tableaux, something that has long been desired by combinatorialists even in the standard case. When $r = 2$, the map from rectangular fluctuating tableaux to fixed-point free involutions given by $T \mapsto \text{prom}_1(T)$ is injective. Indeed, after combining vertices as described above the image is precisely the *non-crossing matchings*. For $r = 3$, a very similar model for semistandard tableaux was considered by Hopkins and Rubey [HR22].

For representation-theoretic purposes, it would be nice to have such a diagrammatic model that naturally extends the dihedral action to a full \mathfrak{S}_n -action. Recall from Remark 6.15 that we do not have a characterization of promotion permutations in general. Therefore, for general r , we do not know how to use this model to define a natural \mathfrak{S}_n -action that extends promotion and evacuation on the span of tableaux. For $r = 3$, the model can be enriched to a web basis for SL_3 [Kup96], which carries a full \mathfrak{S}_n -action (see also, [PPR09, PP21]). In [GPPSS23a], we similarly use this model with $r = 4$ as a starting point to construct a web basis for SL_4 , which again has a full \mathfrak{S}_n -action with σ acting by *rot* and w_0 acting by *refl*. See Figure 8 for an example.

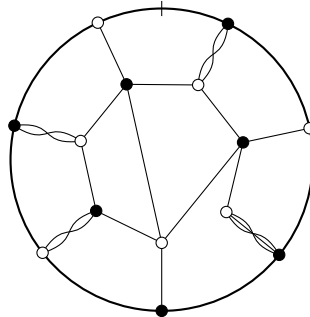


FIGURE 8. The SL_4 -web corresponding to the fluctuating tableau T from Figure 2, as constructed in our companion paper [GPPSS23a].

8. CONNECTIONS TO CRYSTALS

We now give a representation-theoretic interpretation of the promotion functions from Section 6 and reduced promotion matrices from Section 5 by relating fluctuating tableaux to vertices in crystal graphs. Crystal bases were first introduced by Kashiwara [Kas90] (see also, Lusztig [Lus90a]) and are a combinatorial tool to study representations of quantum groups associated to Lie algebras. See [HK02, BS17] for textbook accounts.

8.1. Crystal basics. We largely follow [BS17]. Let Φ be a *root system* for a Euclidean space with positive-definite inner product $\langle -, - \rangle$, Φ^+ a choice of *positive roots*, $\Lambda \supset \Phi$ a *weight lattice*, and $\Sigma = \{\alpha_i : i \in I\} \subset \Phi^+$ a set of *simple roots* with index set I as in [BS17, §2.1]. We require only finite seminormal Kashiwara crystals, which simplifies the exposition.

Definition 8.1. A (finite, seminormal, Kashiwara) *crystal* is a nonempty finite set \mathcal{B} together with maps

$$\begin{aligned} e_i, f_i : \mathcal{B} &\rightarrow \mathcal{B} \sqcup \{0\} & \forall i \in I, \\ \text{wt} : \mathcal{B} &\rightarrow \Lambda \end{aligned}$$

where $0 \notin \mathcal{B}$ is an auxiliary element and which satisfy the following axioms.

(A1) If $x, y \in \mathcal{B}$, then $e_i(x) = y \Leftrightarrow f_i(y) = x$ and

$$\text{wt}(y) = \text{wt}(x) + \alpha_i.$$

(A2) For $x \in \mathcal{B}$, the *i-root string* through x is the collection $\{e_i^k(x), f_i^k(x) : k \geq 0\} \cap \mathcal{B}$. If x is the maximal element in its *i-root string*, i.e. $e_i(x) = 0$, we require the *i-string length*, i.e. the maximal k such that $f_i^k(x) \neq 0$, to be $\langle \text{wt}(x), \alpha_i^\vee \rangle$ where $\alpha^\vee := 2\alpha/\langle \alpha, \alpha \rangle$.

In type A , axiom (A2) says that a basis element $x \in \mathcal{B}$ of weight $\text{wt}(x) = \mu$ which is maximal in its *i-root string* has *i-string length* $\mu_i - \mu_{i+1} \geq 0$. In particular, if x is of *highest weight*, meaning $e_i(x) = 0$ for all $i \in I$, then $\mu_1 \geq \dots \geq \mu_r$ and μ is *dominant*.

Definition 8.2. If \mathcal{B} is a crystal, the *crystal graph* of \mathcal{B} is the labeled, directed graph with vertex set \mathcal{B} and edges $x \xrightarrow{i} y$ whenever $y = f_i(x) \in \mathcal{B}$.

The maps e_i may be recovered from the crystal graph and (A1), so the crystal graph together with the weight function wt entirely encodes the crystal. The edges of \mathcal{B} are oriented “downwards” with respect to the partial order on Λ . One may infer wt from the weights of the set of highest weight elements,

$$\text{hw}(\mathcal{B}) := \{x \in \mathcal{B} : \forall i \in I, e_i(x) = 0\}.$$

A *strict morphism* of crystals is a partially defined map $\mathcal{B} \rightarrow \mathcal{C}$ which preserves wt and sends *i-root strings* bijectively onto *i-root strings*. See [BS17, §4.5] for the formal, general definition. We will only encounter strict morphisms.

Remark 8.3. For the sake of completeness we briefly describe the correspondence between crystals and representation theory. We will not discuss the technical assumptions necessary to make this correspondence precise.

- ♦ Connected components of $\mathcal{B} \longleftrightarrow$ irreducible decomposition of W
- ♦ Highest weight elements of $\mathcal{B} \longleftrightarrow$ dominant weights of the irreducible components of W
- ♦ Weight generating function of $\mathcal{B} \longleftrightarrow$ character of W
- ♦ Tensor product of crystals \longleftrightarrow tensor product of representations
- ♦ Isomorphic crystals \longleftrightarrow isomorphic representations

In particular, connected crystals coming from representation theory are entirely determined by their unique highest weight element, and \mathcal{B} is uniquely determined by $\text{hw}(\mathcal{B})$.

The following crystals correspond to the $\text{GL}_r(\mathbb{C})$ -representations $\bigwedge^k V$ and $\bigwedge^k V^*$; see [BS17, §2.2]. These are the representations that are important for fluctuating tableaux (see Section 2.2).

Example 8.4. In type A_{r-1} , the crystal graph $\mathcal{B}(V)$ of the r -dimensional standard representation V of $\mathrm{GL}_r(\mathbb{C})$ is

$$\boxed{1} \xrightarrow{1} \boxed{2} \xrightarrow{2} \cdots \xrightarrow{r-1} \boxed{r}, \quad \text{where } \mathrm{wt}(\boxed{i}) = \mathbf{e}_i.$$

The unique highest weight element is $\boxed{1}$ of weight \mathbf{e}_1 .

Example 8.5. The crystal graph $\mathcal{B}(V^*)$ of the dual V^* is

$$\boxed{\bar{r}} \xrightarrow{r-1} \boxed{\overline{r-1}} \xrightarrow{r-2} \cdots \xrightarrow{1} \boxed{\bar{1}}, \quad \text{where } \mathrm{wt}(\boxed{\bar{i}}) = -\mathbf{e}_i.$$

The unique highest weight element is $\boxed{\bar{r}}$ of weight $-\mathbf{e}_r$.

Example 8.6. The crystal graph of the exterior power $\bigwedge^k V$ of the standard representation of $\mathrm{GL}_r(\mathbb{C})$ has vertex set

$$\mathcal{B}\left(\bigwedge^k V\right) = \left\{ \begin{array}{c} \boxed{j_1} \\ \boxed{j_2} \\ \vdots \\ \boxed{j_k} \end{array} : 1 \leq j_1 < j_2 < \cdots < j_k \leq r \right\}.$$

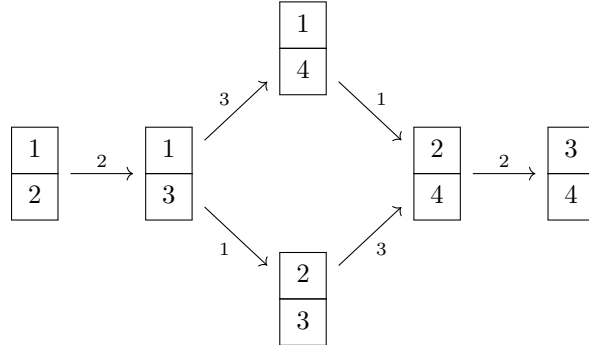
Given a column $C \in \mathcal{B}(\bigwedge^k V)$, we can apply f_i to C by changing i into $i+1$ as long as C does not already contain $i+1$. The weight of C is $\sum_{j \in C} \mathbf{e}_j$. The unique highest weight element is the column consisting of $1, 2, \dots, k$ with weight $\omega_k := \mathbf{e}_1 + \cdots + \mathbf{e}_k$.

Example 8.7. The crystal graph of the dual exterior power $\bigwedge^k V^*$ of the standard representation of $\mathrm{GL}_r(\mathbb{C})$ has vertex set

$$\mathcal{B}\left(\bigwedge^k V^*\right) = \left\{ \begin{array}{c} \boxed{\bar{j}_k} \\ \vdots \\ \boxed{\bar{j}_2} \\ \boxed{\bar{j}_1} \end{array} : 1 \leq j_1 < j_2 < \cdots < j_k \leq r \right\}.$$

Given a column $\bar{C} \in \mathcal{B}(\bigwedge^k V^*)$, we can apply f_i to \bar{C} by changing $\overline{i+1}$ into \bar{i} as long as \bar{C} does not already contain \bar{i} . The weight of \bar{C} is $\sum_{\bar{j} \in \bar{C}} -\mathbf{e}_j$. The unique highest weight element is the column consisting of $\bar{r}, \bar{r-1}, \dots, \bar{r-k+1}$ with weight $\bar{\omega}_k = -\mathbf{e}_r - \cdots - \mathbf{e}_{r-k+1}$.

Example 8.8. When $r = 4, k = 2$, the crystal graph $\mathcal{B}(\bigwedge^2 V)$ is



In general, the *dual* of a crystal graph is obtained by reversing the arrows and negating the weights; see [BS17, Def. 2.20].

Here, we have written columns C or \overline{C} as sets for brevity. The root strings in $\mathcal{B}(\bigwedge^k V)$ are each of length 1, so we only need to consider single brackets in each tensor factor here. This basis element is simultaneously highest and lowest weight, i.e. all f_i, e_i send it to 0. This example is based on the fluctuating tableau from Figure 2.

We may drop the tensor product symbols and identify elements of $\mathcal{B}(\bigwedge^{\underline{c}} V)$ with words whose letters are subsets of \mathcal{A}_r , which appeared in Section 2.4 and Section 2.5. Under this identification, as we now show, highest-weight elements of $\mathcal{B}(\bigwedge^{\underline{c}} V)$ are precisely the lattice words of fluctuating tableaux of type \underline{c} whose weight and final shape coincide. This perspective gives a crystal-theoretic proof of Theorem 2.4.

Proposition 8.14. *Let $\underline{c} = (c_1, \dots, c_n)$ with $c_i \in \{0, \pm 1, \dots, \pm r\}$. Then*

$$\text{hw} \left(\mathcal{B} \left(\bigwedge^{\underline{c}} V \right) \right) = L(\text{FT}(r, n, \underline{c})).$$

Proof. Recall that lattice words L of fluctuating tableaux are characterized by the inequalities (2.2). Concretely, in each prefix of L , we require the number of a 's minus the number of \overline{a} 's to be weakly greater than the number of b 's minus the number of \overline{b} 's for all $1 \leq a \leq b \leq r$. We may equivalently restrict these conditions to the case where $a = i, b = i + 1$ for $1 \leq i \leq r - 1$.

Now, consider a highest-weight word L . In order for e_i to result in 0, the bracketing rule must result in no unmatched $\overline{] }$'s. Equivalently, in each prefix of the sequence of brackets, there must be at least as many $[$'s as $\overline{] }$'s. The $[$'s arise precisely from letters containing $(i \text{ but not } i + 1)$ or $(\overline{i} + \overline{1} \text{ but not } \overline{i})$. The $\overline{] }$'s arise precisely from letters containing $i + 1$ but not i or \overline{i} but not $\overline{i} + \overline{1}$. It is straightforward that these conditions are equivalent to the conditions on lattice words. \square

The same argument shows that the *lowest* weight elements of $\mathcal{B}(\bigwedge^{\underline{c}} V)$ are precisely the *reverse* lattice words, namely those where in every *suffix* the number of i 's minus the number of \overline{i} 's is at *most* the number of $i + 1$'s minus the number of $\overline{i} + \overline{1}$'s. In particular, rectangular fluctuating tableaux are special in the following sense.

Corollary 8.15. *The isolated vertices of $\mathcal{B}(\bigwedge^{\underline{c}} V)$, i.e. the simultaneous highest and lowest weight elements, are precisely the rectangular fluctuating tableaux of type \underline{c} .*

8.4. Crystals, oscillization, and switch. We may interpret oscillization from Section 2.6 as arising from a crystal morphism. First, we have a map

$$\mathcal{B} \left(\bigwedge^k V \right) \rightarrow \mathcal{B}(V)^{\otimes k}$$

given by sending $\{i_1 < \dots < i_k\}$ to $i_1 \otimes \dots \otimes i_k$. There is an analogous dual notion sending $\{\overline{i}_1 < \dots < \overline{i}_k\}$ to $\overline{i}_1 \otimes \dots \otimes \overline{i}_k$ with highest weight $\{\overline{r}, \dots, \overline{r - k + 1}\} \mapsto \overline{r} \otimes \dots \otimes \overline{r - k + 1}$. We leave the proof of the following to the reader.

Lemma 8.16. *Let $\underline{c} = (c_1, \dots, c_n)$ with $c_i \in \{0, \pm 1, \dots, \pm r\}$ and let $\text{osc}(\underline{c})$ be the sequence where c_i is replaced by $|c_i|$ copies of 1 if $c_i \geq 0$ and $\overline{1}$ if $c_i \leq 0$. The oscillization map*

$$\text{osc}: \text{FT}(r, \lambda, \underline{c}) \rightarrow \text{FT}(r, \lambda, \text{osc}(\underline{c}))$$

is the inclusion on highest-weight elements induced by the crystal inclusion

$$\mathcal{B} \left(\bigwedge^{\underline{c}} V \right) \rightarrow \mathcal{B} \left(\bigwedge^{\text{osc}(\underline{c})} V \right).$$

The switch maps from Definition 3.2 similarly arise from the crystal isomorphisms

$$\begin{aligned} \mathcal{B}\left(\bigwedge^c V\right) &\xrightarrow{\sim} \mathcal{B}\left(\det(V) \otimes \bigwedge^{r-c} V^*\right) \\ \{i_1 < \dots < i_c\} &\mapsto \{1, \dots, r\} \otimes \{\bar{j}_1 < \dots < \bar{j}_{r-c}\} \\ \mathcal{B}\left(\bigwedge^c V^*\right) &\xrightarrow{\sim} \mathcal{B}\left(\det(V^*) \otimes \bigwedge^{r-c} V\right) \\ \{\bar{i}_1 < \dots < \bar{i}_c\} &\mapsto \{\bar{r}, \dots, \bar{1}\} \otimes \{j_1 < \dots < j_{r-c}\} \end{aligned}$$

where $\{i_1, \dots, i_c\} \sqcup \{j_1, \dots, j_{r-c}\} = [r]$. In terms of lattice words, we may freely add or remove the letters $\{1, \dots, r\}$ or $\{\bar{r}, \dots, \bar{1}\}$ without materially altering the combinatorics of the preceding sections.

8.5. Crystals and promotion. We now describe crystal-theoretic interpretations of the Bender–Knuth involutions (following Lenart [Len08]) and promotion (following Pfannerer–Rubey–Westbury [PRW20]). We then give a different crystal-theoretic “balance point” description of promotion (Proposition 8.22), as well as a crystal-theoretic interpretation of reduced promotion matrices (Theorem 8.24).

Although $\mathcal{B} \otimes \mathcal{C} \cong \mathcal{C} \otimes \mathcal{B}$, the naive map $x \otimes y \mapsto y \otimes x$ does not respect the bracketing rule and is not generally a morphism of crystals. Henriques–Kamnitzer [HK06] introduced *crystal commutators*

$$\sigma_{\mathcal{B}, \mathcal{C}}: \mathcal{B} \otimes \mathcal{C} \rightarrow \mathcal{C} \otimes \mathcal{B}.$$

These are natural involutive crystal isomorphisms that make the category of crystals into a *coboundary category*. There is a corresponding action of the *n-fruit cactus group* on *n*-fold tensor products of crystals. See [Len08, §2.4] for details. We will not require the specifics of these constructions until Section 8.6.

Lenart [Len08] interpreted the local rules of van Leeuwen [vL98] in terms of crystal commutators. Specifically, we have the following.

Theorem 8.17 ([Len08, Thm. 4.4]). *The bijection on highest weight elements induced by*

$$\sigma_{\mathcal{B}(\bigwedge^{\underline{c}} V), \mathcal{B}(\bigwedge^{\underline{d}} V)}: \mathcal{B}\left(\bigwedge^{\underline{c}} V\right) \otimes \mathcal{B}\left(\bigwedge^{\underline{d}} V\right) \xrightarrow{\sim} \mathcal{B}\left(\bigwedge^{\underline{d}} V\right) \otimes \mathcal{B}\left(\bigwedge^{\underline{c}} V\right)$$

is given by the $|\underline{c}| \times |\underline{d}|$ growth diagram

$$\begin{array}{ccc} \lambda & \xrightarrow{\underline{d}} & \nu \\ \underline{c} \uparrow & & \uparrow \underline{c} \\ \emptyset & \xrightarrow{\underline{d}} & \mu \end{array}$$

Proof. One may reduce to the transpose semistandard case using the **switch** involutions and the naturality of the crystal commutator. In that setting, the theorem is a direct restatement of [Len08, Thm. 4.4] into our terminology. \square

In particular, promotion has the following crystal-theoretic description, as observed in [PRW20, §4]. Recall we may identify a fluctuating tableau T with its lattice word $L(T)$.

Corollary 8.18. *Let $\underline{c} = (c_1, \underline{d})$ and $\underline{c}' = (\underline{d}, c_1)$. The bijection on highest weight elements induced by*

$$\sigma_{\mathcal{B}(\bigwedge^{c_1} V), \mathcal{B}(\bigwedge^{\underline{d}} V)}: \mathcal{B}\left(\bigwedge^{\underline{c}} V\right) \rightarrow \mathcal{B}\left(\bigwedge^{\underline{c}'} V\right)$$

is given by promotion \mathcal{P} on fluctuating tableaux of type \underline{c} .

Remark 8.19. Let G be a Lie group with a representation U and corresponding crystal graph \mathcal{B} . A more general version of Corollary 8.15 (cf. [Wes18]) states that a basis of $\text{Inv}_G(U^{\otimes n})$ is indexed by the isolated vertices in the crystal $\mathcal{B}^{\otimes n}$, which are often identified with various kinds of tableaux. In particular,

- ♦ for the adjoint representation of GL_r , these vertices are *Stembridge’s alternating tableaux* [Ste87];
- ♦ for the vector representation of Sp_{2r} these are *Sundaram’s r -symplectic oscillating tableaux* [Sun90];
- ♦ for the vector representation of $\text{SO}(2r+1)$ these are *vacillating tableaux* [Jag19];
- ♦ and the spin representation of $\text{Spin}(2r+1)$ these are *r -fans of Dyck paths* [PPSS23].

Corollary 8.18 motivates a definition of promotion on such kinds of tableaux using the crystal commutator $\sigma_{\mathcal{B}, \mathcal{B}^{\otimes(n-1)}}$. A description of promotion in terms of local rules using Theorem 8.17 is then possible whenever the representation U can be embedded in a tensor product of minuscule representations. In the definition from Equation (3.2) of the local rules, **sort** needs to be replaced with the function that maps a weight to the unique dominant representative in its Weyl group orbit. All of the families of tableaux listed above may be embedded in the set of fluctuating tableaux using identifications coming from virtual crystal morphisms. Hence, promotion on fluctuating tableaux extends promotion on all of the other families listed above. See [Wes18, PRW20, PPSS23, HSW23] for further discussion of promotion in other Lie types.

It will be convenient to 0-index some lattice words, contrary to our earlier convention.

Proposition 8.20. *Let $w_0 \dots w_{n-1} \in \text{FT}(n, r, \underline{c})$. To compute $\mathcal{P}(w_0 \dots w_{n-1})$, do the following.*

- (i) *Delete w_0 .*
- (ii) *Apply raising operators e_i to $w_1 \dots w_{n-1}$ to reach a highest weight element $w'_1 \dots w'_{n-1}$.*
- (iii) *Append the unique element $w'_n \in \mathcal{B}(\bigwedge^{c_1} V)$ such that the weight of $w_0 \dots w_{n-1}$ agrees with the weight of $w'_1 \dots w'_{n-1} w'_n$.*

Proof. Corollary 8.18 explains the relation between promotion of fluctuating tableaux and crystal commutators. The rest of the proposition is a special case of the description from [PRW20, Cor. 4.19] of crystal commutators on highest weight elements of tensor products of crystals. \square

The intermediate steps of the “raising algorithm” in Proposition 8.20 do not obviously correspond to the intermediate steps in the computation of promotion via Bender–Knuth involutions as in Example 4.10. Nonetheless, using the bracketing rule, we may give a more explicit combinatorial description of this crystal-theoretic promotion algorithm when $|c_1| = 1$.

Definition 8.21. Let $w_0 \dots w_{n-1} \in \text{FT}(n, r, \underline{c})$ be the lattice word of a fluctuating tableau and let $0 \leq a \leq n-1$. An *i -balance point starting from a* is an index $j \geq a$ such that, in the subword $w_a w_{a+1} \dots w_j$, the number of i ’s minus the number of \bar{i} ’s equals the number of $i+1$ ’s minus the number of $\overline{i+1}$ ’s. We call the difference $\#i - \#\bar{i} - \#(i+1) + \#\overline{i+1}$ the *slack* of the index j with respect to i and a . The index j is an *i -balance point starting from a* if and only if its slack with respect to i and a is 0.

Proposition 8.22. *Let $w := w_0 \dots w_{n-1} \in \text{FT}(n, r, \underline{c})$ with $|c_1| = 1$. Suppose the raising operators in Proposition 8.20 acting on $w_1 \dots w_{n-1}$ and resulting in the highest weight element $w'_1 \dots w'_{n-1}$ are, in order, e_{i_1}, \dots, e_{i_k} , acting on positions j_1, \dots, j_k .*

Then we have the following:

- ♦ *If $c_1 = 1$, then $i_1, \dots, i_k = 1, 2, \dots, k$ and $w'_n = k+1$.*
- ♦ *If $c_1 = -1$, then $i_1, \dots, i_k = r-1, r-2, \dots, r-k$ and $w'_n = \overline{r-k}$.*

For convenience, set $j_0 := 0$ and $i_{k+1} := k+1$ if $c_1 = 1$ and $i_{k+1} := r-k-1$ if $c_1 = -1$. Then, for each $1 \leq h \leq k$, j_h is the first i_h -balance point of w starting at j_{h-1} . There is no i_{k+1} -balance point of w starting at j_k . In particular, the sequence $1 \leq j_1 \leq \dots \leq j_k \leq n-1$ weakly increases, and in the rectangular case, $k = r-1$.

Proof. Let $w = w_0 w_1 \dots w_{n-1} \in \text{FT}(n, r, \underline{c})$. We assume $c_1 = 1$, the case $c_1 = -1$ being similar. Consider applying e_i to w by writing $[_i$'s and $]_i$'s below appropriate letters. Since w is a highest weight word, every $]_i$ is matched with a $[_i$. In particular, the number of $[_i$'s in any prefix is at least as great as the number of $]_i$'s. The difference between these two numbers is the slack, as in Definition 8.21. Since $w_0 = 1$ has $[_1$, it is matched in w with the $]_1$ at the first 1-balancing point of w , say $j_1 \geq 1$, if it exists. Cutting away w_0 , the brackets $[_i$ and $]_i$ for $w' := w_1 \dots w_{n-1}$ with $i > 1$ are unchanged from those in w , hence fully matched, and the only raising operator which may possibly apply to w' is e_1 . Indeed, e_1 applies to w' precisely at position j_1 , which we may assume exists, since otherwise we are done.

Let w'' be the result of applying e_1 to w' at w_{j_1} . We have two cases.

- ◆ Suppose w_{j_1} has $2 \in w_{j_1}$, $1 \notin w_{j_1}$, and is decorated with $]_1$ and $]_2$ in w . Applying e_1 results in 1 , which is decorated with $]_1$ in w'' .
- ◆ Suppose w_{j_1} has $\bar{1} \in w_{j_1}$, $\bar{2} \notin w_{j_1}$, and is decorated with $]_1$ and $]_2$ in w . Applying e_1 results in $\bar{2}$, which is decorated with $]_1$ and $]_2$ in w'' .

In particular, we see that w'' has no unmatched $]_1$'s or $]_i$'s for $i > 2$, since w has none. As for $i = 2$, the $]_2$'s and $]_2$'s in w'' are the same as those in w except that the $]_2$ at w_{j_1} has been deleted and possibly replaced with $]_2$. Since e_2 applies to the rightmost unmatched $]_2$, in either case we see that e_2 applies to w'' at the $]_2$ matched with the $]_2$ of w_{j_1} in w if it exists, which is at j_2 , the first 2-balance point starting at j_1 . Continuing in this way, we see inductively that $i_1, \dots, i_k, j_1, \dots, j_k$, and k are as described.

In the rectangular case, the reverse word is also a lattice word, so the reverse lattice condition implies that, for all i , each suffix $w_a w_{a+1} \dots w_{n-1}$ has an i -balanced subword $w_a w_{a+1} \dots w_j$, so the necessary balance points always exist. \square

When applying the raising algorithm in Proposition 8.20 when $|c_1| = 1$, Proposition 8.22 shows that there is a unique crystal raising path. When $|c_1| > 1$, however, there are generally multiple possible paths. Nonetheless, we may oscillize the $\bigwedge^{c_1} V$ and repeatedly apply Proposition 8.22, which gives a deterministic calculation, as in the following example.

Example 8.23. Let $w = \{12\}\bar{4}\{134\}2\{\bar{32}\}\{34\}\bar{1}$ be the lattice word of the fluctuating tableau from Figure 2, where $r = 4$. Oscillizing the first letter and applying each of Proposition 8.20 and Proposition 8.22 twice yields

$$\begin{array}{ll}
\{12\}\bar{4}\{134\}2\{\bar{32}\}\{34\}\bar{1} & \bar{1}\bar{4}\{124\}2\{\bar{42}\}\{34\}\bar{1}\bar{4} \\
\stackrel{\text{osc}}{\rightarrow} \bar{1}2\bar{4}\{134\}2\{\bar{32}\}\{34\}\bar{1} & \stackrel{\text{cut}}{\rightarrow} \bar{4}\{124\}2\{\bar{42}\}\{34\}\bar{1}\bar{4} \\
\stackrel{\text{cut}}{\rightarrow} \bar{2}\bar{4}\{134\}2\{\bar{32}\}\{34\}\bar{1} & \stackrel{e_1}{\rightarrow} \bar{4}\{124\}1\{\bar{42}\}\{34\}\bar{1}\bar{4} \\
\stackrel{e_1}{\rightarrow} \bar{1}\bar{4}\{134\}2\{\bar{32}\}\{34\}\bar{1} & \stackrel{e_3}{\rightarrow} \bar{4}\{124\}1\{\bar{42}\}\{24\}\bar{1}\bar{4} \\
\stackrel{e_3}{\rightarrow} \bar{1}\bar{4}\{124\}2\{\bar{32}\}\{34\}\bar{1} & \stackrel{e_3}{\rightarrow} \bar{4}\{124\}1\{\bar{42}\}\{24\}\bar{1}\bar{3} \\
\stackrel{e_3}{\rightarrow} \bar{1}\bar{4}\{124\}2\{\bar{42}\}\{34\}\bar{1} & \stackrel{\text{app}}{\rightarrow} \bar{4}\{124\}1\{\bar{42}\}\{24\}\bar{1}\bar{3}\bar{4} \\
\stackrel{\text{app}}{\rightarrow} \bar{1}\bar{4}\{124\}2\{\bar{42}\}\{34\}\bar{1}\bar{4} & \stackrel{\text{osc}^{-1}}{\rightarrow} \bar{4}\{124\}1\{\bar{42}\}\{24\}\bar{1}\{34\}
\end{array}$$

Here, we have highlighted in blue each tensor factor that is being acted on.

Consequently, $\mathcal{P}(\{12\}\bar{4}\{134\}2\{\bar{32}\}\{34\}\bar{1}) = \bar{4}\{124\}1\{\bar{42}\}\{24\}\bar{1}\{34\}$, in agreement with the calculation from Example 3.9 by Bender–Knuth involutions.

Alternatively, we could cut away $\{12\}$ entirely and apply the raising algorithm in Proposition 8.20 directly. The corresponding crystal operations occur in a crystal isomorphic to Example 8.8, where two possible paths could be taken. The analogue of the path from the oscillization calculation is the

path that applies e_2, e_3, e_1, e_2 in that order to $w_1 \dots w_6 = \overline{4}\{134\}2\{\overline{32}\}\{34\}\overline{1}$ at positions 2, 4, 3, 5, respectively.

By the next result, we may use this path to determine the non-diagonal entries in the top rows of the reduced promotion matrices $\overline{\mathbf{M}}^1(T)$, $\overline{\mathbf{M}}^2(T)$, and $\overline{\mathbf{M}}^3(T)$ from Example 5.21. For example, the e_2 is applied at positions 2 and 5, resulting in 1's in those columns (indexed starting at 0) of the top row of $\overline{\mathbf{M}}^2(T)$ and 0's elsewhere.

We now give a crystal-theoretic interpretation of reduced promotion matrices, strengthening the link between crystals and promotion permutations.

Theorem 8.24. *Let T be an r -row fluctuating tableau of length n . Fix $1 \leq j \leq n-1$.*

Then $\overline{\mathbf{M}}^i(T)_{u, u+j}$ (with the column index $u+j$ taken modulo n) is the number of times the raising operator e_i is applied at index j of the lattice word $L(\mathcal{P}^{u-1}(T))$ when computing the promotion of $\mathcal{P}^{u-1}(T)$ by the raising algorithm in Proposition 8.20.

Proof. It suffices to consider a single local rule diagram as in Proposition 5.19.

$$\begin{array}{ccc} \lambda & \longrightarrow & \nu \\ \uparrow & \overline{\mathbf{M}}^i & \uparrow \\ \kappa & \longrightarrow & \mu \end{array}$$

where $\lambda = \kappa + \mathbf{e}_A$, $\nu = \mu + \mathbf{e}_B$, $\mu = \kappa + \mathbf{e}_U$, $\nu = \lambda + \mathbf{e}_V$ and $\overline{\mathbf{M}}^i$ are the reduced promotion matrix entries.

Now, the top edge corresponds to the letter V in a crystal word and the bottom edge corresponds to the letter U . If e_i is applied to V a total of m_i times during the crystal raising algorithm, then

$$(8.2) \quad \mathbf{e}_V = \mathbf{e}_U + \sum_{i=1}^{r-1} m_i(\mathbf{e}_{i+1} - \mathbf{e}_i).$$

The entries of $\overline{\mathbf{M}}^i$ are uniquely determined from A and B by (5.5) in Proposition 5.19. Since $\mathbf{e}_B - \mathbf{e}_A = \mathbf{e}_V - \mathbf{e}_U$, the theorem then follows by the uniqueness in Proposition 5.19, comparing (5.5) to (8.2). \square

8.6. Crystals and a fundamental involution. The involution ε from Section 2.5 may be interpreted in terms of crystals using Lusztig's involution. We sketch this connection here.

Lusztig's involution [Lus90b] is a certain involution η on crystals that sends elements of weight α to elements of weight $\text{rev} \circ \alpha$; see [HK06, §2.2] or [PRW20, §4.1] for details. In particular, η acts on $\mathcal{B}(\bigwedge^c V)$ by “complementing” elements, i.e. by sending $\pm S \subseteq [r]$ to $\pm\{r+1-s : s \in S\}$. Lusztig's involution interchanges the unique highest and lowest weight elements of a connected crystal.

Theorem 8.25. *On lattice words of r -row fluctuating tableaux, we have*

$$(8.3) \quad \eta \circ \mathcal{E} = \varepsilon = \mathcal{E}^* \circ \eta.$$

Proof. Henriques–Kamnitzer [HK06] defined an action of the n -fruit cactus group on n -fold tensor products of crystals. The n -fruit cactus group is a certain group generated by elements $s_{p,q}$ for intervals $[p, q] \subseteq [n]$. By [HK06, p.207], the action can be defined on words by

$$s_{p,q}(w_1 \dots w_n) = w_1 \dots w_{p-1} \eta(\eta(w_q) \dots \eta(w_p)) w_{q+1} \dots w_n.$$

The involution ε reverses words and complements letters. Thus,

$$s_{p,q}(w_1 \dots w_n) = w_1 \dots w_{p-1} \eta(\varepsilon(w_p \dots w_q)) w_{q+1} \dots w_n.$$

In particular, $s_{1,n} = \eta \circ \varepsilon$ on $\mathcal{B}(\bigwedge^c V)$.

The special case $s_{p,p+1}$ corresponds to acting on the p th and $(p+1)$ st factors of $\bigwedge^c V$ by the crystal commutators from Section 8.5, fixing the other factors. By [PRW20, Lem. 4.2] and Lenart's

Theorem 8.17, $s_{1,n}(L) = \mathcal{E}(L)$ when L is the lattice word of a fluctuating tableau of length n . Hence $\mathcal{E} = \eta \circ \varepsilon$, so $\eta \circ \mathcal{E} = \varepsilon$. Using Lemma 3.13(iii), we also have

$$\mathcal{E}^* = \varepsilon \circ \mathcal{E} \circ \varepsilon = \varepsilon \circ \eta.$$

The theorem follows. \square

Since Lusztig's involution is the identity on isolated vertices, which are precisely the rectangular fluctuating tableaux, an alternate proof of Theorem 6.5 is as an immediate corollary of (8.3).

ACKNOWLEDGEMENTS

This project began during the 2021 BIRS Dynamical Algebraic Combinatorics program hosted at UBC Okanagan, and we are very grateful for the excellent research environment provided there. At that conference, Sam Hopkins and Martin Rubey introduced us to the notion of prom_1 for rectangular standard tableaux. We also wish to thank Rebecca Patrias and Anne Schilling for their helpful comments. Part of this work was done at NDSU, for whose hospitality we are very thankful. Finally, we are grateful for the resources provided at ICERM, where this paper was completed.

REFERENCES

- [BK72] Edward A. Bender and Donald E. Knuth, *Enumeration of plane partitions*, J. Combinatorial Theory Ser. A **13** (1972), 40–54.
- [BPS16] Jonathan Bloom, Oliver Pechenik, and Dan Saracino, *Proofs and generalizations of a homomesy conjecture of Propp and Roby*, Discrete Math. **339** (2016), no. 1, 194–206.
- [BS17] Daniel Bump and Anne Schilling, *Crystal bases: representations and combinatorics*, World Scientific Publishing Co. Pte. Ltd., Hackensack, NJ, 2017.
- [CGP20] Michael Chmutov, Max Glick, and Pavlo Pylyavskyy, *The Berenstein-Kirillov group and cactus groups*, J. Comb. Algebra **4** (2020), no. 2, 111–140.
- [GPPSS23a] Christian Gaetz, Oliver Pechenik, Stephan Pfannerer, Jessica Striker, and Joshua P. Swanson, *Rotation-invariant web bases from hourglass plabic graphs*, preprint (2023), 60 pages, [arXiv:2306.12501](#).
- [GPPSS23b] Christian Gaetz, Oliver Pechenik, Stephan Pfannerer, Jessica Striker, and Joshua P. Swanson, *An SL_4 -web basis from hourglass plabic graphs*, Sémin. Lothar. Combin. **89B** (2023), Art. 9, 12 pages.
- [Hai92] Mark D. Haiman, *Dual equivalence with applications, including a conjecture of Proctor*, Discrete Math. **99** (1992), no. 1-3, 79–113.
- [HK02] Jin Hong and Seok-Jin Kang, *Introduction to quantum groups and crystal bases*, Graduate Studies in Mathematics, vol. 42, American Mathematical Society, Providence, RI, 2002.
- [HK06] André Henriques and Joel Kamnitzer, *Crystals and coboundary categories*, Duke Math. J. **132** (2006), no. 2, 191–216.
- [HR22] Sam Hopkins and Martin Rubey, *Promotion of Kreweras words*, Selecta Math. (N.S.) **28** (2022), no. 1, Paper No. 10, 38 pages.
- [HSW23] Graeme Henrickson, Anna Stokke, and Max Wiebe, *A cyclic sieving phenomenon for symplectic tableaux*, preprint (2023), 16 pages, [arXiv:2303.09605](#).
- [Jag19] Judith Jagenteufel, *A Sundaram type bijection for $SO(2k+1)$: vacillating tableaux and pairs consisting of a standard Young tableau and an orthogonal Littlewood-Richardson tableau*, preprint (2019), 48 pages, [arXiv:1902.03843](#).
- [Kas90] Masaki Kashiwara, *Crystalizing the q -analogue of universal enveloping algebras*, Comm. Math. Phys. **133** (1990), no. 2, 249–260.
- [KK99] Mikhail Khovanov and Greg Kuperberg, *Web bases for $\mathfrak{sl}(3)$ are not dual canonical*, Pacific J. Math. **188** (1999), no. 1, 129–153.
- [KR84] Joseph P. S. Kung and Gian-Carlo Rota, *The invariant theory of binary forms*, Bull. Amer. Math. Soc. (N.S.) **10** (1984), no. 1, 27–85.
- [Kup96] Greg Kuperberg, *Spiders for rank 2 Lie algebras*, Comm. Math. Phys. **180** (1996), no. 1, 109–151.
- [Len08] Cristian Lenart, *On the combinatorics of crystal graphs. II. The crystal commutator*, Proc. Amer. Math. Soc. **136** (2008), no. 3, 825–837.
- [Lus90a] G. Lusztig, *Canonical bases arising from quantized enveloping algebras*, J. Amer. Math. Soc. **3** (1990), no. 2, 447–498.
- [Lus90b] G. Lusztig, *Canonical bases arising from quantized enveloping algebras. II*, no. 102, 1990, Common trends in mathematics and quantum field theories (Kyoto, 1990), pp. 175–201 (1991).
- [Pat19] Rebecca Patrias, *Promotion on generalized oscillating tableaux and web rotation*, J. Combin. Theory Ser. A **161** (2019), 1–28.

- [Pec14] Oliver Pechenik, *Cyclic sieving of increasing tableaux and small Schröder paths*, J. Combin. Theory Ser. A **125** (2014), 357–378.
- [PP21] Rebecca Patrias and Oliver Pechenik, *Tableau evacuation and webs*, preprint (2021), 10 pages.
- [PPR09] T. Kyle Petersen, Pavlo Pylyavskyy, and Brendon Rhoades, *Promotion and cyclic sieving via webs*, J. Algebraic Combin. **30** (2009), no. 1, 19–41.
- [PPSS23] Joseph Pappe, Stephan Pfannerer, Anne Schilling, and Mary Claire Simone, *Promotion and growth diagrams for fans of Dyck paths and vacillating tableaux*, preprint (2023), 41 pages, [arXiv:2212.13588](#).
- [PRW20] Stephan Pfannerer, Martin Rubey, and Bruce Westbury, *Promotion on oscillating and alternating tableaux and rotation of matchings and permutations*, Algebr. Comb. **3** (2020), no. 1, 107–141.
- [Rho10] Brendon Rhoades, *Cyclic sieving, promotion, and representation theory*, J. Combin. Theory Ser. A **117** (2010), no. 1, 38–76.
- [RSSW01] Tom Roby, Frank Sottile, Jeff Stroomer, and Julian West, *Complementary algorithms for tableaux*, J. Combin. Theory Ser. A **96** (2001), no. 1, 127–161.
- [Rus13] Heather M. Russell, *An explicit bijection between semistandard tableaux and non-elliptic sl_3 webs*, J. Algebraic Combin. **38** (2013), no. 4, 851–862.
- [Sch72] M. P. Schützenberger, *Promotion des morphismes d’ensembles ordonnés*, Discrete Math. **2** (1972), 73–94.
- [Spe14] David E. Speyer, *Schubert problems with respect to osculating flags of stable rational curves*, Algebr. Geom. **1** (2014), no. 1, 14–45.
- [Sta99] Richard P. Stanley, *Enumerative combinatorics. Vol. 2*, Cambridge Studies in Advanced Mathematics, vol. 62, Cambridge University Press, Cambridge, 1999, With a foreword by Gian-Carlo Rota and appendix 1 by Sergey Fomin.
- [Sta09] Richard P. Stanley, *Promotion and evacuation*, Electron. J. Combin. **16** (2009), no. 2, Special volume in honor of Anders Björner, Research Paper 9, 24 pages.
- [Ste87] John R. Stembridge, *Rational tableaux and the tensor algebra of gl_n* , J. Combin. Theory Ser. A **46** (1987), no. 1, 79–120.
- [Ste02] John R. Stembridge, *A concise proof of the Littlewood-Richardson rule*, Electron. J. Combin. **9** (2002), no. 1, Note 5, 4 pages.
- [Sun90] Sheila Sundaram, *Orthogonal tableaux and an insertion algorithm for $SO(2n+1)$* , J. Combin. Theory Ser. A **53** (1990), no. 2, 239–256.
- [TL71] H. N. V. Temperley and E. H. Lieb, *Relations between the “percolation” and “colouring” problem and other graph-theoretical problems associated with regular planar lattices: some exact results for the “percolation” problem*, Proc. Roy. Soc. London Ser. A **322** (1971), no. 1549, 251–280.
- [Tym12] Julianna Tymoczko, *A simple bijection between standard $3 \times n$ tableaux and irreducible webs for \mathfrak{sl}_3* , J. Algebraic Combin. **35** (2012), no. 4, 611–632.
- [vL98] Marc A. A. van Leeuwen, *An analogue of jeu de taquin for Littelmann’s crystal paths*, Sémin. Lothar. Combin. **41** (1998), Art. B41b, 23 pp.
- [Wes18] Bruce W. Westbury, *Coboundary categories and local rules*, Electron. J. Combin. **25** (2018), no. 4, Paper No. 4.9, 22 pages.

(Gaetz) DEPARTMENT OF MATHEMATICS, CORNELL UNIVERSITY, ITHACA, NY, USA.

Email address: crgaetz@gmail.com

(Pechenik) DEPARTMENT OF COMBINATORICS & OPTIMIZATION, UNIVERSITY OF WATERLOO, ON, CANADA.

Email address: oliver.pechenik@uwaterloo.ca

(Pfannerer) INSTITUTE OF DISCRETE MATHEMATICS AND GEOMETRY, TECHNISCHE UNIVERSITÄT WIEN, AUSTRIA.

Email address: stephan.pfannerer@tuwien.ac.at

(Striker) DEPARTMENT OF MATHEMATICS, NORTH DAKOTA STATE UNIVERSITY, FARGO, ND, USA.

Email address: jessica.striker@ndsu.edu

(Swanson) DEPARTMENT OF MATHEMATICS, UNIVERSITY OF SOUTHERN CALIFORNIA, LOS ANGELES, CA, USA.

Email address: swansonj@usc.edu